The Structure and Function of Frataxin

**Krisztina Z. Bencze,
Kalyan C. Kondapalli,
Jeremy D. Cook, and
Stephen McMahon**
Department of Biochemistry
and Molecular Biology, Wayne
State University, School of
Medicine, Detroit, Michigan,
USA

**César Millán-Pacheco and
Nina Pastor**
Facultad de Ciencias,
Universidad Autonoma del
Estado de Morelos,
Cuernavaca, Morelos, Mexico

Timothy L. Stemmler
Department of Biochemistry
and Molecular Biology, Wayne
State University, School of
Medicine, Detroit, Michigan,
USA

Address correspondence to Timothy L. Stemmler, Department of Biochemistry and Molecular Biology, Wayne State University, School of Medicine, 540 E. Canfield Ave, Detroit, Michigan 48201, USA. E-mail: tstemmle@med.wayne.edu

ABSTRACT   Frataxin, a highly conserved protein found in prokaryotes and eukaryotes, is required for efficient regulation of cellular iron homeostasis. Humans with a frataxin deficiency have the cardio- and neurodegenerative disorder Friedreich's ataxia, commonly resulting from a GAA trinucleotide repeat expansion in the frataxin gene. While frataxin's specific function remains a point of controversy, the general consensus is that the protein assists in controlling cellular iron homeostasis by directly binding iron. This review focuses on the structural and biochemical aspects of iron binding by the frataxin orthologs and outlines molecular attributes that may help explain the protein's role in different cellular pathways.
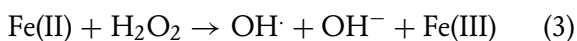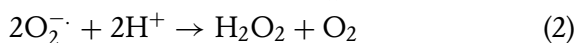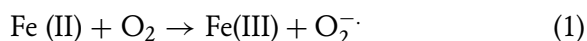
Keywords: Friedreich's ataxia, heme biosynthesis, iron-sulfur cluster assembly, iron chaperone, Yfh1, CyaY, ferrochelatase, ISU, Aconitase
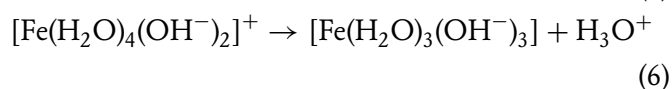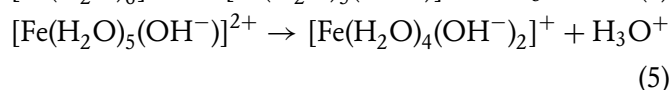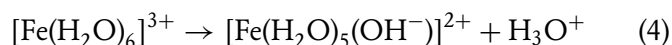
INTRODUCTION

Frataxin, a conserved protein found ubiquitously in prokaryotes and eukaryotes, is required for the cellular regulation of iron homeostasis. Although of extreme interest to many chemists and biologists alike, frataxin's exact role in helping cells regulate iron chemistry and metal availability remains controversial at best. Frataxin has been proposed to participate in at least five different capacities: 1) as an iron chaperone during cellular heme and iron-sulfur (Fe-S) cluster production; 2) as an iron-storage protein during conditions of iron overload; 3) as an aid in the repair of oxidatively damaged aconitase Fe-S clusters; 4) as a factor that controls cellular oxidative stress by moderating the concentration of reactive oxygen species (ROS); and finally 5) as an active participant in pathways involving energy conversion and oxidative phosphorylation. While these functions are not necessarily exclusive, it seems extraordinary that one protein could directly control so many biological pathways within cells. Disruption of frataxin production does cause a general loss in the cellular control of iron bioavailability and reactivity; however, phenotypes are complicated, a fact that further inhibits definition of the protein's exact function. The goal of this manuscript is to take a structural approach to help readers understand frataxin's role during the regulation of cellular iron homeostasis. However, before we begin to draw structural correlations regarding frataxin's function, it is beneficial to first look in detail at the iron chemistry the protein helps control.

Iron is extremely versatile in the chemistry it can perform, so it is no surprise that the metal is found ubiquitously in all living systems. Iron is found in the active sites of proteins involved in many diverse cellular functions, ranging from oxygen transport, oxidative metabolism, and electron transport to energy production. Iron's ability to cycle between the ferrous (Fe[II]) and ferric (Fe[III]) oxidation states allows the metal to be extremely useful when performing redox chemistry, and "this chemical versatility is surely a reason why nature selected this element in so many life processes" (Cotton *et al.*, 1988). Unfortunately iron's flexibility toward performing redox chemistry means that the metal, if left unregulated, can perform deleterious reactions that elevate ROS concentrations, and these reactive oxygen species can damage cells by oxidatively attacking cellular membranes, proteins, and DNA alike. Ferrous iron will readily react with dioxygen to produce superoxide and ultimately hydroxyl radicals, as described by the Fenton reaction (Aisen *et al.*, 2001; Kosman, 2003):

$$\text{Fe (II)} + O_2 \rightarrow \text{Fe(III)} + O_2^{-\cdot} \quad (1)$$

$$2O_2^{-\cdot} + 2H^+ \rightarrow H_2O_2 + O_2 \quad (2)$$

$$\text{Fe(II)} + H_2O_2 \rightarrow OH^\cdot + OH^- + \text{Fe(III)} \quad (3)$$

It is therefore beneficial to control the oxidation of ferrous iron as a means to prevent the damaging effects of hydroxyl radical production. Under normal physiological conditions (pH > 2), ferric iron undergoes stepwise hydrolysis leading to the formation of insoluble neutral species:

$$[\text{Fe}(H_2O)_6]^{3+} \rightarrow [\text{Fe}(H_2O)_5(OH^-)]^{2+} + H_3O^+ \quad (4)$$

$$[\text{Fe}(H_2O)_5(OH^-)]^{2+} \rightarrow [\text{Fe}(H_2O)_4(OH^-)_2]^+ + H_3O^+ \quad (5)$$

$$[\text{Fe}(H_2O)_4(OH^-)_2]^+ \rightarrow [\text{Fe}(H_2O)_3(OH^-)_3] + H_3O^+ \quad (6)$$

Organisms have therefore evolved protein-controlled mechanisms to modulate iron's redox chemistry. These mechanisms allow cells to adapt quickly to enhancement or suppression of iron import, delivery of Fe for utilization, and finally the storage of this important element for future use. In humans, iron abstracted from diet is reduced and acidified by the low-pH environment of the stomach, and a portion is eventually transported for use in the production of heme and Fe-S clusters. A small percentage of the metal is also stored in a manner that can be easily mobilized. More than two thirds of the iron found in the body is incorporated into hemoglobin in developing erythroid precursor cells or in mature red blood cells (Andrews, 1999), highlighting the importance of heme Fe-prosthetic groups as components that help control local O_2 concentration, availability, and reactivity. Owing to their remarkable structural plasticity and versatile chemical/electronic features, Fe-S clusters are additional prosthetic groups that help control cell and organism viability by participating in electron transfer events, substrate binding and activation, iron and sulfur storage, the regulation of gene expression, and in some cases enzyme activity (Johnson *et al.*, 2005). The balance of iron in biological systems, however, is fragile, as both iron deficiency and overload are destructive to cells. Diseases related to the disruption in cellular iron homeostasis are, as a result, among the most common diseases found in humans.

Friedreich's ataxia (FRDA), an autosomal recessive cardio- and neurodegenerative disorder that affects 1 in 50,000 humans, results from an inability to produce frataxin, and causes protein deficiency that leads to a disruption of cellular iron homeostasis (Delatycki *et al.*, 2000). The majority of patients with FRDA (~96%) have extensive trinucleotide repeat expansions in the first intron of the gene encoding frataxin, while a small percentage of patients have frataxin point mutations (Campuzano *et al.*, 1996). The expanded GAA repeat adopts abnormal DNA structures that impair frataxin transcription; the longer the repeat, the more profound the frataxin deficiency, the earlier the onset of the disorder, and the greater the intensity of the disease (Bidichandani *et al.*, 1998; Ohshima *et al.*, 1998; Pandolfo, 2002). In humans, frataxin is a 210-amino-acid protein that is nuclear encoded but has an N-terminal mitochondrial targeting sequence that is removed during processing (Campuzano *et al.*, 1996; Gibson *et al.*, 1996). Results from immunocytofluorescence and immunocytoelectron microscopy show processed frataxin is predominately located within the mitochondria and associated with mitochondrial membranes, crests and as free soluble protein within the matrix (Gibson *et al.*, 1996). Frataxin mRNA is predominantly expressed in tissues with a high metabolic rate, including the liver, kidney, neurons and heart (Koutnikova *et al.*, 1997). Phenotypes coupled with frataxin deficiency include mitochondrial iron

K. Z. Bencze et al.

accumulation (Babcock *et al.*, 1997; Foury *et al.*, 1997), disruption in both heme and Fe-S cluster production (Rotig *et al.*, 1997; Stehling *et al.*, 2004) and a progressive breakdown in cellular iron homeostasis (Babcock *et al.*, 1997; Koutnikova *et al.*, 1997). Mitochondrial iron accumulation diverts metal away from other cellular compartments and frataxin deficient cells accommodate for what they perceive as a general cellular iron deficiency by elevating mitochondrial iron import (Babcock *et al.*, 1997). Boosting pathways that lead to increased mitochondrial iron import facilitates the problems associated with not being able to process the reactive iron that is already present, leading to further elevation in ROS levels, gradual cell damage and finally the loss of cell viability (Delatycki *et al.*, 2000). FRDA patients therefore show a slow progression of muscular and neurological symptoms (loss of motor function, progressive limb and gait ataxia, *etc.*) linked to the disruption in proper iron regulation and the disorder is typically fatal due to complications resulting from cardiomyopathy (Orth *et al.*, 2001).

A direct correlation between frataxin and cellular iron homeostasis is at present obvious, but early studies on the yeast frataxin homolog (Yfh1) provided the initial insight into what role(s) frataxin may play in helping cells maintain iron homeostasis (Babcock *et al.*, 1997). Deletion of the frataxin gene results in the accumulation of mitochondrial iron deposits (Babcock *et al.*, 1997; Foury *et al.*, 1997) coupled with both aconitase and general Fe-S cluster protein deficiencies (Foury, 1999; Rotig *et al.*, 1997). The presence of zinc suppresses iron accumulation phenotypes in yeast (Knight *et al.*, 1998). ΔYfh1 cells were shown to be hypersensitive to H_2O_2, iron and copper levels (Babcock *et al.*, 1997; Foury *et al.*, 1997). Based on the observation that reintroduction of Yfh1 expression under depleted conditions can promote the recovery and export of these mitochondrial iron deposits, frataxin was originally proposed to directly control mitochondrial iron efflux (Radisky *et al.*, 1999). Yfh1 was also shown to indirectly regulate mitochondrial iron uptake by interacting and partially controlling the activity of the yeast mitochondrial intermediate peptidase (YMIP), a metalloprotease required for maturation of ferrochelatase and other iron utilizing proteins (Branda, Yang *et al.*, 1999).

In eukaryotes, frataxin is proteolytically processed during the production of the mature soluble protein found within the mitochondrial matrix. During translation, a frataxin precursor is produced which contains a N-terminal targeting sequence that directs the protein to the mitochondria and eventually into the matrix (Babcock *et al.*, 1997; Knight *et al.*, 1998). Processing of the yeast frataxin precursor protein takes place uniquely in two steps (Branda *et al.*, 1999; Gordon *et al.*, 2001). Typically, proteins targeted to the mitochondria are processed in a single step (Branda *et al.*, 1999; Cavadini *et al.*, 2000; Gordon *et al.*, 2001). There are only a few additional proteins that show this variation; examples include the Rieske (Fe-S) containing proteins and *Neurospora crassa* ATPase subunit 9 (Branda *et al.*, 1999; Cavadini *et al.*, 2000; Gordon *et al.*, 2001). Even within this category, only frataxin and ATPase subunit 9 use a single enzyme for processing during both steps (Cavadini *et al.*, 2000). In the first step, the mitochondrial processing peptidase removes the N-terminal 20 residues (domain I) of the protein, generating a Yfh1 intermediate. This intermediate is then processed again by the peptidase to remove the next 31 amino acids (domain II), generating the 123 amino acid mature Yfh1 found within the matrix. The two processing steps are independent. Domain I is a typical mitochondrial targeting signal and it can be substituted by other mitochondrial targeting signals with similar cellular results. Domain II serves as a spacer. The first 20 amino acids of frataxin contain the 5 basic residues typically found in mitochondrial targeting signals. The N-terminal region of the mature protein is rich in acidic residues. A spacer separates basic residues in the targeting signal from acidic residues in the mature protein's N-terminus. This prevents unwanted interactions that might hinder recognition of the target signal by the import proteins. Both domains are required for import into the mitochondria; however, protein with mutations blocking the first or second processing steps will still complement the Yfh1 deletion phenotype (Gordon *et al.*, 2001).

N-terminal processing of human frataxin (HsFtx) is still a matter of debate. Cavadini and colleagues (2000) proposed a two-step processing of the N-terminus, whereas Gordon and coworkers could identify only a single processing event (Gordon *et al.*, 2001). In the two-step processing proposal, the first cleavage occurs between residues 41 and 42, removing the first 41 residues of HsFtx to generate an intermediate. The second cleavage step occurs between residues 55 and 56, removing only the next 14 N-terminal residues. The kinetics of the first processing step were

The Structure and Function of Frataxin

shown to be similar between the different species, however the second cleavage reaction rate is species specific. The second processing step (*i.e.,* removing the 14 residues) is the rate-limiting step during HsFtx processing (Cavadini, Adamec *et al.*, 2000). In contrast, Gordon and coworkers (2001) detected only a single processing event generating the 18 kDa mature human frataxin and similar results were observed with rat or yeast mitochondrial peptidase.

STRUCTURAL INSIGHTS INTO FRATAXIN'S FUNCTION

A detailed understanding of frataxin's structure provides some insight into how the protein may function within its different proposed roles. Specific questions relevant to the molecular structure of frataxin include: Is there a patch of residues that could accommodate iron binding if frataxin is acting as a metal chaperone? Is there a favorable interface that could promote contacts between frataxin and protein partners coupled with heme biosynthesis, Fe-S cluster assembly, and aconitase Fe-S cluster repair? Are there molecular elements on frataxin's surface that might promote protein aggregation during an iron storage function? And finally, does frataxin support an active site that could assist in the stabilization of the redox chemistry performed by the bound iron? We will attempt to address each question by looking closely at the structures of the different frataxin orthologs.

Solution and crystal structures have been reported for the yeast, human and bacterial (CyaY) frataxin orthologs (Cho *et al.*, 2000; Dhe-Paganon *et al.*, 2000; He *et al.*, 2004; Lee *et al.*, 2000; Musco *et al.*, 2000; Nair *et al.*, 2004). Frataxin has a unique fold that combines two terminal α-helices to make one plane, five antiparallel β-strands that construct the second plane of the protein and a sixth (and, in HsFtx, a seventh) β-strand that intersects the planes to give an overall planar $\alpha-\beta$ sandwich structure motif (Figure 1). The general shared frataxin topology is $\alpha1\beta1\beta2\beta3\beta4\beta5\beta6(\beta7)\alpha2$, strand seven is again only detected in HsFtx. In all three cases, the structures are extremely similar; RMSD's of HsFtx *versus* CyaY and Yfh1 in regions of secondary structure are 1.34 Å and 0.65 Å, respectively. The overall structural dimensions of the orthologs are: 47 $\times$ 32 $\times$ 28 Å^3 for HsFtx, 45 $\times$ 30 $\times$ 25 Å^3 for CyaY and 47 $\times$ 29 $\times$ 23 Å^3 for Yfh1. Mature HsFtx

spans amino acids 75 to 210 of the total expressed sequence, however auto-degradation and proteolysis at the protein's N-terminus prior to $\alpha1$ residues have complicated structural studies of the full-length mature protein. Therefore, the structures solved of HsFtx begin at residue 88 in the crystal structure and at 90 in the solution structure (Dhe-Paganon *et al.*, 2000; Musco *et al.*, 2000). Circular dichroism data on full-length mature HsFtx indicate the N-terminal residues prior to residue 92 are predominately unstructured. Mature Yfh1 spans residues 52 to 174 of the expressed gene sequence. Unlike HsFtx, the 18 amino acids N-terminal to $\alpha1$ in Yfh1 are stable and partially structured in a 3_{10} helix observed between residues 65 and 68. Mature CyaY lacks any appreciable residues N-terminal to $\alpha1$. In the case of HsFtx only, frataxin has a 17 amino acid C-terminal tail following $\alpha2$. This C-terminal tail of HsFtx adopts a random coil structure that is tethered to the protein's helical plane exposed surface.

The strong structural similarity between frataxin orthologs results from the fact that these proteins share an extremely high degree of amino acid sequence similarity. Sequence identity of Yfh1 *versus* both CyaY and HsFtx are 28.1% and 37.8%, respectively, while respective sequence similarities are 59.8% and 65.0%. A large number of the highly conserved amino acids include a subset of Asp and Glu residues located in the N-terminal region of the protein. For Yfh1 this amounts to 9 of the first $\sim$50 N-terminal residues in the mature protein constructed by conserved Asp and Glu residues (Figure 2). Conserved N-terminal acidic residues are located in the $\alpha1$ and $\beta1$ secondary structural regions of frataxin. Electrostatic potential plots show these conserved acidic residues line the exposed surface of the $\alpha1$ and $\beta1$ interfaces, generating a general negatively charged surface that covers roughly a quarter of frataxin's total accessible surface (Dhe-Paganon *et al.*, 2000). Carboxylate side chains from Asp and Glu residues often serve as ligands for bound metal in many iron-binding proteins, suggesting the possibility of these regions participating in metal binding. While HsFtx does not contain any cysteines, CyaY and Yfh1 contain poorly conserved cysteines at positions distant from the acidic patches.

Multiple factors have been shown to influence the stability of frataxin's fold. The Pastore laboratory (MRC, London) performed extensive *in vitro* studies on the three characterized frataxins with the goal of defining factors that help stabilize each protein's
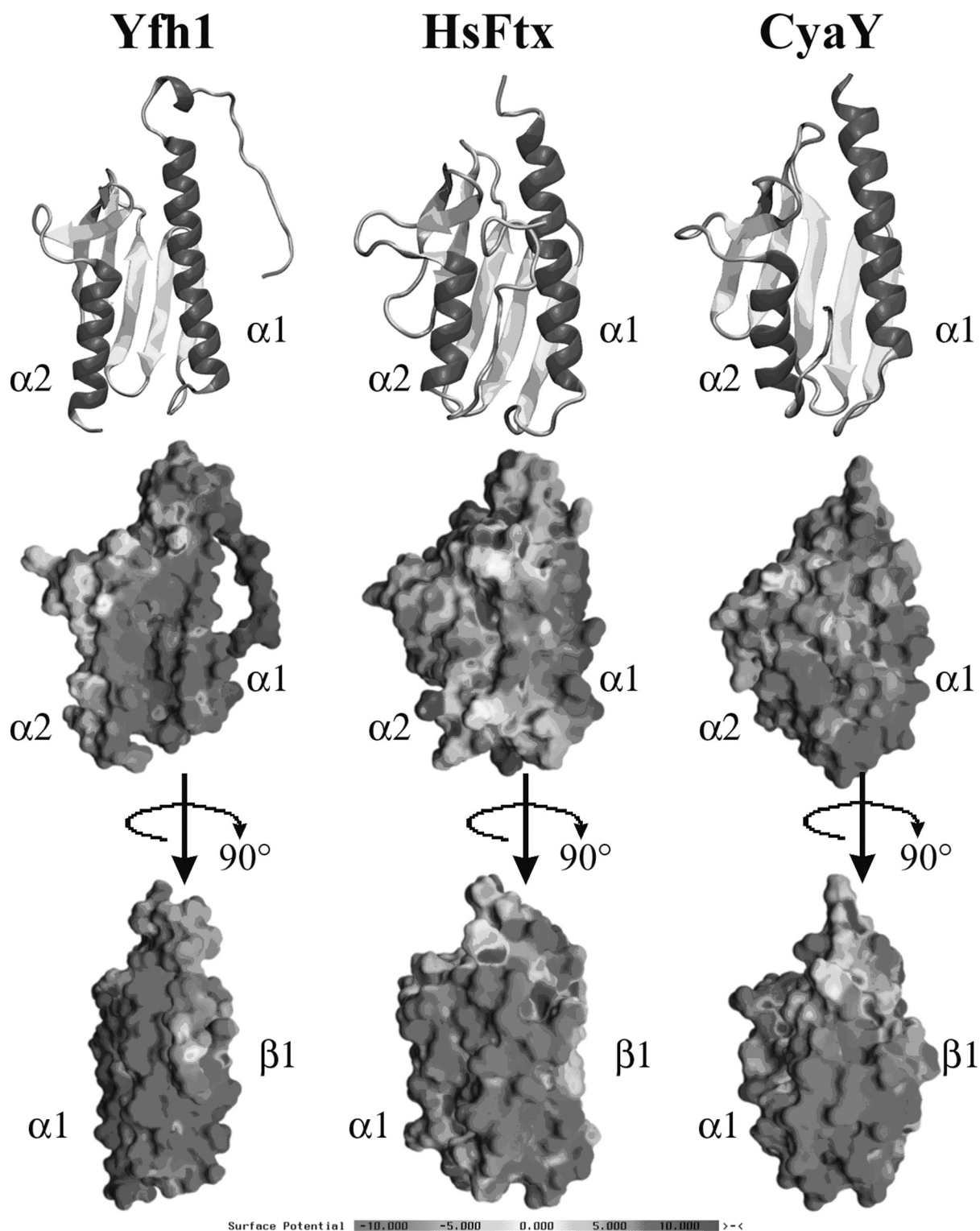
K. Z. Bencze et al.

Figure 1   Top: ribbon diagram for yeast, human and bacterial frataxin. Middle: electropotential plots for proteins in same orientation. Bottom: electropotential plots for proteins rotated -90 degrees around the y-axis compared to top display. Structure figures made using solution structures of Yfh1 (PDB ID# 2GA5), HsFtx (PDB ID# 1LY7) and CyaY (PDB ID# 1SOY) frataxins. (Figure appears in color online at www.crbmb.com)

structure (Adinolfi *et al.*, 2004; Adinolfi *et al.*, 2002). Apo-bacterial, yeast and human frataxin are predominately stable as monomers at 1 mM protein concentrations, as confirmed by proton linewidths observed in ^{15}N labeled protein ^{15}N-HSQC specta (He *et al.*, 2004; Mori, 1995; Musco *et al.*, 1999; Musco *et al.*, 2000; Nair *et al.*, 2003; Nair *et al.*, 2004). Apo-Yfh1 is however stable as a monomer for only up to 2 weeks

The Structure and Function of Frataxin

```
C.elegans       M-------LSTILRNNFV----------------------------------------------------          11
S.pombe         -----MQSLRAAFRRRTPIFLKPYEFST-------------------------------------------N         24
A.thaliana      -----MATASRFLLRKLPRFLKLSPTLL----------RSNGVRVSSNLIQDSIEPLDSFWRIGSRIRHDSLT        58
D.melanogaster  MFA-GRLMVRSIVGRACLATMG------RWSKPQAHASQVILPSTPAIAAV---------------AIQCEE         50
M.musculus      MWAFGGRAAVGLLPR-TASRASAWVGNP-RWREPIVTCGRRGLHVTVNAGAT-RHAHLNLHYL-QILNIKKQS        69
M.fascicularis  MWTFGRRAVAGLLASPSPAQAQTLTRAP-RLAELAQLCSRRGLRTGINATRTTHHTSSNLRGLNQIRNVKRQS        72
H.sapiens       MWTLGRRAVAGLLASPSPAQAQTLTRVP-RPAELAPLCGRRGLRTDIDATCTPRRASSNQRGLNQIWNVKKQS        72
E.coli          ------------------------------------------------------------------------
S.cerevisiae    ---MIKRSLASLVRVSSVMGRRYMIAAAGGERARFCPAVTNKKNHTVN-------------------TFQKR         50
Ruler           ..............................................................50
```

```
                                     :.  ..      :  :  :::       .        *          *:*:  .             .
C.elegans       ----RRSFSSRIFSQN-----EYETAADSTLERLSDYFDQIA--DSFPVSEQFDVSHAMGVLTVNVSKSVGTY        73
S.pombe         VFGLRCRYYSQVRHNGALTDLEYHRVADDTLDVLNDTFEDLL--EEVGK-KDYDIQYANGVITLMLG-EKGTY        93
A.thaliana      TRSFSSQGPASVDYSSVLQEEEFHKLANFTINHLLEKIEDYG---DNVQIDGFDIDYGNEVLTLKLGSLG-TY        127
D.melanogaster  FTANRRLFSSQIETESTLDGATYERVCSDTLDALCDYFEELT--ENASELQGTDVAYSDGVLTVNLGGGQHGTY       121
M.musculus      VCVVHLRNLGTLDNPSSLDETAYERLAEETLDSLAEFFEDLA--DKPYTLEDYDVSFGDGVLTIKLGGDLGTY        140
M.fascicularis  VYLMNLRKSGTLGHPGSLDDTTYERLAEETLDSLAEFFEDLA--DKPYTFEDYDVSFGSGVLTVKLGGDLGTY        143
H.sapiens       VYLMNLRKSGTLGHPGSLDETTYERLAEETLDSLAEFFEDLA--DKPYTFEDYDVSFGSGVLTVKLGGDLGTY        143
E.coli          -----------------MNDSEFHRLADQLWLTIEERLDDW--DGDSDI----DCEINGGVLTITFENG-SKI         49
S.cerevisiae    FVESSTDGQVVPQEVLNLPLEKYHEEADDYLDHLLDSLEELS---EAHPDCIPDVELSHGVMTLEIPAF-GTY        119
Ruler           .........60........70........80........90............100.......110........1
```

```
                                  α1                        β1      β2
```
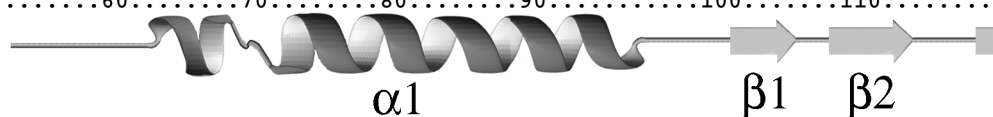
```
                ::*:* *  :*:*:::    .*   :::            *     :      :   :*
C.elegans       VINKQSPNKQIWLSSPMSGPKRYDLEEE---GKWTYAHDGEQLDSLLNREFRKILADDRIDFSRHV------        136
S.pombe         VINKQPPAHQIWLSSPVSGPKHYEYSLKS--KTWCSTRDEGTLLGILSSEFSKWFSR-PIEFKKSEDF----        158
A.thaliana      VLNKQTPNRQIWMSSPVSGPSRFDWDRDA--NAWIYRRTEAKLHKLLEEELENLCGEPIQLS----------        187
D.melanogaster  VINRQTPNKQIWLSSPTSGPKRYDFVGTVAAGRWIYKHSGQSLHELLQQEIPGILKSQSVDFLRLPYCS---        190
M.musculus      VINKQTPNKQIWLSSPSSGPKRYDWTGK----NWVYSHDGVSLHELLARELTKALNT-KLDLSSLAYSGKGT        207
M.fascicularis  VINKQTPNKQIWLSSPSSGPKRYDRTGK----NWVYSHDGVSLHELLGAELTKALKT-KLDLSSLAYSGKDA        210
H.sapiens       VINKQTPNKQIWLSSPSSGPKRYDWTGK----NWVYSHDGVSLHELLAAELTKALKT-KLDLSSLAYSGKDA        210
E.coli          IINRQEPLHQVWLATKQGG-YHFDLKG----DEWICDRSGETFWDLLEQAATQQAGET-VSFR---------        106
S.cerevisiae    VINKQPPNKQIWLASPLSGPNRFDLLN----GEWVSLRNGTKLTDILTEEVEKAISKS-Q-----------        174
Ruler           20.......130.......140...........150.......160.......170................
```

```
          β3          β4          β5          β6          α2
```
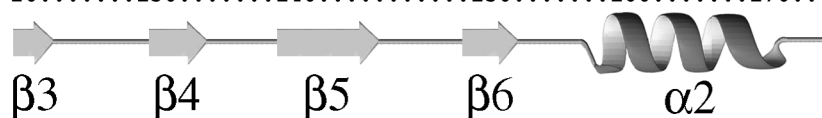
Figure 2 ClustalX alignment for a subset of characterized frataxin orthologs. Bottom three sequences represent structurally characterized frataxin orthologs. Secondary structural elements and ruler representing Yfh1 properties are given below the sequences.

after isolation, at which point it begins to self aggregate (Cook *et al.*, 2006). Although CyaY, Yfh1 and HsFtx share a high degree of sequence homology and fold, the bacterial and human orthologs have melting points in the respective range of 54°C and 60°C (Adinolfi *et al.*, 2004), while the yeast protein is less stable, with a melting point at 39°C (Adinolfi *et al.*, 2004 and unpublished results from our laboratory). The type of buffer (organic *vs.* phosphate) has minimal effect on protein stability for these three frataxin orthologs, however the presence of salt generally increases the stability of frataxin's fold (most pronounced in Yfh1). Lowering the pH raised the stability of Yfh1 but this had no effect on the helical fold of CyaY and HsFtx within the pH range of 6 to 8. The presence of iron at high

metal to protein stoichiometries further increased the stability of all frataxin orthologs. Residues C-terminal to α2 in the protein's structure appear to dramatically increase the general stability of frataxin. C-terminal CyaY truncation mutants matching the shorter Yfh1 construct showed a substantial (14°C) drop in the protein's melting temperature. A C-terminal extension to Yfh1 caused a ∼7°C increase in the protein's melting temperature. Structural studies show the C-terminal extension in CyaY and HsFtx are unstructured but make surface contacts with α1 and α2 amino acids, most likely providing additional contacts that help stabilize the protein's fold. Finally, the non-conserved N-terminal region of full-length HsFtx appears to be important for the partial apo-protein aggregation often

K. Z. Bencze et al.

RIGHTSLINK

found in the *in vitro* expressed/isolated protein (O'Neill *et al.*, 2005).

Close inspection of frataxin's helical plane shows interesting structural attributes that may contribute to a better understanding of how the protein binds metal and also of mutations that cause FRDA (Delatycki *et al.*, 2000). On Yfh1, α1 is lined with surface exposed acidic residues Glu71, Asp78, Asp79, Asp82, Asp86, Glu89, Glu90 and Glu93 (Figure 3A). The orientation and proximity of these conserved residues
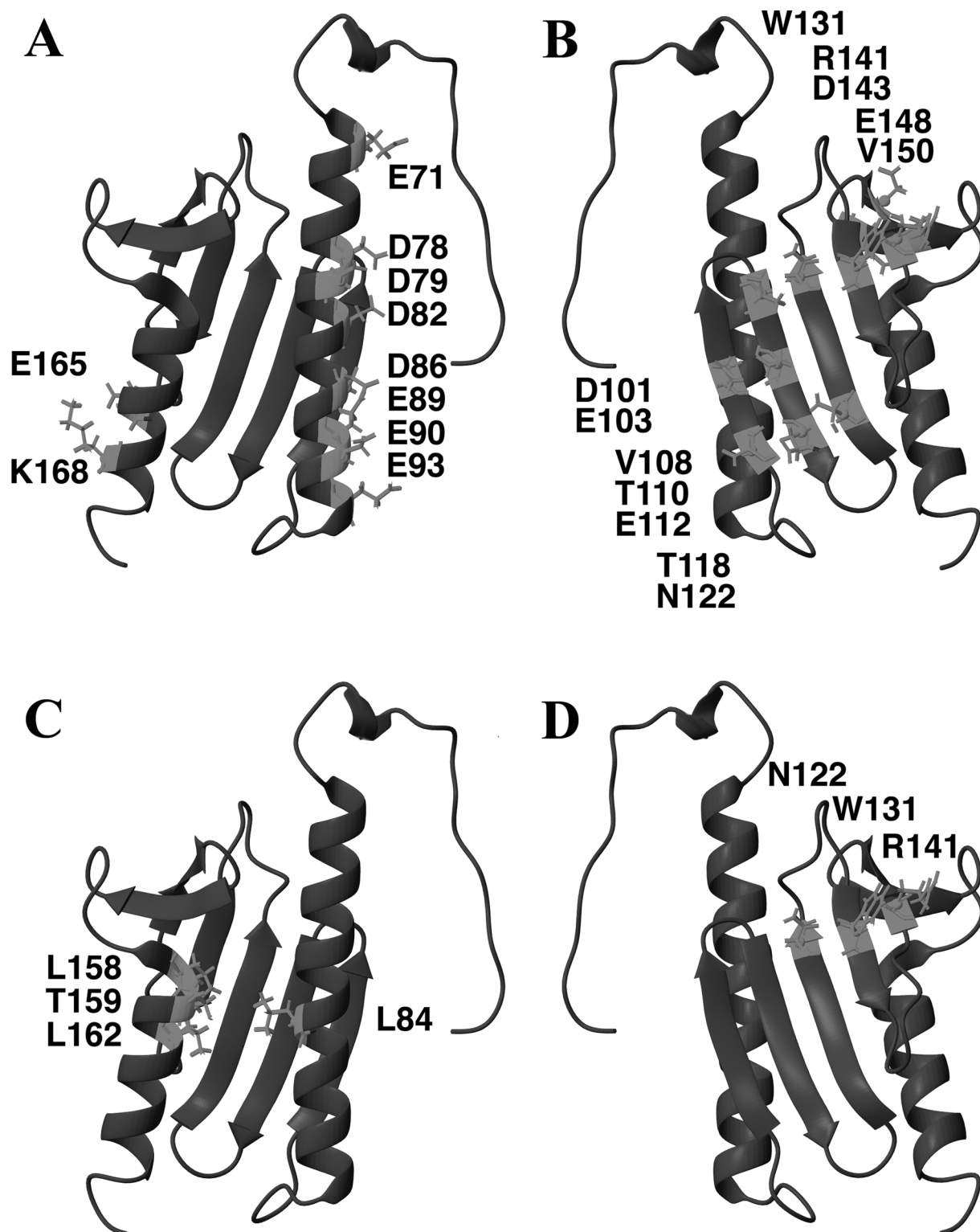

Figure 3 Yfh1 residues that are highly conserved on the helical (A) and β-sheet (B) planes of the protein. Identity of HsFtx FRDA point mutations on the helical (C) and β-sheet (D) planes of Yfh1. Structure figures made using Yfh1 solution structure (PDB ID# 2GA5).

The Structure and Function of Frataxin

generates a conserved acidic patch on the protein in this region and these residues would be in a perfect position to contribute to cation binding. Frataxin helices $\alpha 1$ and $\alpha 2$ are parallel and oriented at an average adjacent backbone distance of ~ 11 Å, predominately due to interactions between the long side chains of hydrophobic and aromatic residues within this plane (in Yfh1, $\alpha 1$ residues in this region include Leu84, Leu88, and Leu91 and $\alpha 2$ residues include Leu162, Val166 and Ile170). Additional interactions between hydrophobic core amino acids on the β-sheet surface of the protein help secure the spatial orientation of $\alpha 1$ to $\alpha 2$. In case of the human frataxin, the C-terminal tail of HsFtx, including residues Thr196, Leu198, and Leu200, appear to further contribute to the stabilization of these inter-helical residue interactions (Cho et al., 2000; Dhe-Paganon et al., 2000; Lee et al., 2000; Musco et al., 2000; Nair et al., 2004). Surface exposed residues on the $\alpha 2$ surface of frataxin are less conserved; in Yfh1, Glu165, and Lys168 are fairly well conserved however the remaining surface residues are mixed. Yfh1 surface residues in the $\beta 6$-loop (or in HsFtx $\beta 6$-$\beta 7$) region share highly conserved polar Arg153 and Asn154 residues. Disease-causing HsFtx helical plane point mutations are identified on the conserved Yfh1 sequence as $\alpha 1$ residue Leu84 mutation (to a Ser) and on $\alpha 2$, Leu158 mutation (to a His), Thr159 mutation (to an Arg) and Leu162 mutation (to an Arg) (Figure 3C) (Bartolo et al., 1998; Cossee et al., 1999; Filla, 1996; Zuhlke et al., 2004). Since these are all buried in the globular domain of the protein and play an important role in the packing of the two helices, mutating these residues most likely causes a disruption of elements that stabilize frataxin's fold.

Numerous surface exposed residues on the β-sheet plane of frataxin are also highly conserved, and close inspection of this surface aids in the understanding of mutations that cause FRDA. Surface exposed residues on the Yfh1 β-sheet plane include Asp101, Glu103, Val108, Thr110, Glu112, Thr118, Asn122, Trp131, Arg141, Asp143, Glu148 and Val150, of which Asp101, Thr110, Asn122, Trp131, and Asp143 are fully conserved (Figure 3B). HsFtx amino acids, complementary in position to Yfh1 residues Asn122, Trp131 and Arg141, are surface exposed and mutated in a small set of FRDA patients (Figure 3D) (Forrest et al., 1998; Labuda et al., 1999; Zuhlke et al., 2004). Yfh1 β-sheet residues with side chains directed towards the hydrophobic core of frataxin include the conserved

residues Ile121, Leu132 and Trp149. Along the β-sheet surface of HsFtx, Yfh1 residues at complementary positions of Ile130, Leu132 and Trp149 were found as point mutations in some FRDA patients, and mutating these residues would surely alter frataxin's fold (Campuzano et al., 1996; Cossee et al., 1999). In addition, Gly107 in the loop region between Yfh1's $\beta 1$ and $\beta 2$ is an additional point mutation found in a subset of FRDA patients (Bidichandani et al., 1997). Yfh1 residue Ile99 is the final HsFtx point mutation seen in a subset of FRDA patients, and this residue is located on the β-sheet plane of frataxin, connecting $\alpha 1$ to $\beta 1$ (Cossee et al., 1999).

Although frataxin's fold is fairly unique, an $\alpha-\beta$ sandwich motif structure is seen in a surprising number of proteins that share similar functions to those proposed for frataxin. The $\alpha-\beta$ sandwich motif can be easily recognized in the ferredoxin-like fold of some cytosolic copper chaperones. Although human HAH1 (Anastassopoulou et al., 2004), yeast ATX1 (Arnesano et al., 2001), and BsCopZ (Banci et al., 2003) (PDB ID's: 1TL5, 1FES and 1P8G) are smaller in their overall size compared to frataxin (ca. 18Å × 22Å × 30 Å), and their helices are tilted at 45° to each other, the helices and beta strands still form a general two-layer structure that is similar to the $\alpha-\beta$ sandwich motif found in frataxin. The copper binding domains of these proteins involve a conserved CXXC motif in a loop region; this binding site is surrounded by hydrophobic residues that are essential for binding to partner proteins but distinct in position from the acidic patch on frataxin's $\alpha 1/\beta 1$ surface (i.e., the proposed metal binding region of frataxin). Recent crystallographic data on complex I of the *Thermus thermophilus* mitochondrial respiratory chain revealed a previously unknown protein Nqo15 that is also a member of this superfamily (Sazanov et al., 2006). Nqo15 binds in close contact with four other domains to help stabilize the larger complex. This protein is constructed by 129 amino acids, held together in an $\alpha-\beta$ sandwich motif fold. Despite a low sequence homology (average of 12%), the crystal structures superimpose well with RMSD values of 2.5 Å and 3.3 Å for CyaY and HsFtx, respectively. This domain binds to the complex through its β-sheet surface in a manner that creates a hydrophilic channel connecting the solvent with the N3 subdomain. The N-terminal $\beta 1$ and loop connecting $\beta 1$ and $\beta 2$ contain several surface exposed histidine residues. Based on the fold similarity between frataxin and Nqo15, and

K. Z. Bencze et al.

a recent publication from the Cowan laboratory (Ohio State University) that proposed frataxin's β-sheet plane may be an essential interface when interacting with ISU proteins during Fe-S cluster assembly (Yoon *et al.*, 2003), the authors of the Nqo15 structure proposed that the conserved β-sheet plane histidine residues could serve as an iron binding site during iron storage and delivery by the protein when reconstitution of the Fe-S cluster in subdomain N3 is required.

FRATAXIN'S IRON BINDING ABILITY

Given the spatial arrangement of conserved acidic residues on the α1/β1 regions of frataxin (Figure 1), and the fact that Asp and Glu carboxylate side chains are chemically suited as ligands for binding metals, it is not surprising to learn that frataxin is an iron binding protein. However, the Isaya laboratory (Mayo Clinic) was the first to identify that frataxin directly binds iron; this iron binding ability was first determined in the yeast system (Adamec *et al.*, 2000). The iron binding ability of additional frataxin orthologs has since been confirmed for both the human and bacterial proteins (Adinolfi *et al.*, 2002; Bou-Abdallah *et al.*, 2004; Cavadini *et al.*, 2002; Cook *et al.*, 2006; Yoon *et al.*, 2003; Yoon *et al.*, 2004). While it was initially recognized that iron binding in the yeast system induces frataxin to oligomerize under unique solution conditions, numerous subsequent reports suggest that oligomerization is not essential when the protein functions in an iron chaperone capacity (*i.e.*, during heme and Fe-S cluster assembly), but it may be important when the protein participates in helping control ROS production under iron overloading conditions. In an attempt to deconvolute the published reports concerning the iron binding ability of frataxin in its different oligomeric states and to determine how these relate to the different proposed functions of frataxin, we will selectively discuss, in the following text, issues concerning: first, the iron binding ability of monomeric frataxin; second, frataxin's ability to form iron loaded oligomers; and finally the protein's ability to regulate the redox chemistry performed by iron bound to the protein. Each of these points is summarized below.

Frataxin Will Bind Iron as a Stable Protein Monomer

Metal to protein stoichiometries, measured for monomeric bacterial, yeast and N-terminally truncated human frataxin show these proteins will tightly bind 2, 2 and 7 Fe(II) atoms, respectively (Bou-Abdallah *et al.*, 2004; Cook *et al.*, 2006; Yoon *et al.*, 2003). Iron dissociation constants, measured for CyaY, Yfh1 and N-terminally truncated HsFtx give average K_d values of 3.8, 3.0 and 55.0 μM, respectively (Bou-Abdallah *et al.*, 2004; Cook *et al.*, 2006; Yoon *et al.*, 2003). The presence of magnesium or calcium salts, at physiologically relevant concentrations found within the mitochondria, stabilize CyaY and Yfh1 in the iron bound monomeric state against oligomerization, while a large portion of bacterially overexpressed HsFtx is stable as an iron-loaded monomer regardless of the solution conditions (Adinolfi *et al.*, 2002; Cook *et al.*, 2006). N-terminally truncated HsFtx was shown to bind ~6 Fe(III) atoms at a K_d of 10.2 μM (Yoon *et al.*, 2003). In the presence of oxidants, monomeric CyaY can bind up to 6 Fe(III) atoms and will interact with up to 25 Fe(III) atoms/monomer (Bou-Abdallah *et al.*, 2004). Ferric iron binding studies for Yfh1 are linked only to protein homooligomerization (Adamec *et al.*, 2000).

NMR spectroscopy provided a powerful tool for identifying frataxin amino acids directly affected by the presence of iron. Backbone amide resonances for the three characterized frataxins are generally well dispersed, hence providing a fingerprint for the majority of protein amino acids (He *et al.*, 2004; Musco *et al.*, 1999; Nair *et al.*, 2003). Subtle perturbations in the amide resonances and general signal intensity due to the addition of iron therefore serve as markers for residues affected by the presence of paramagnetic iron. Ferrous iron titrations performed anaerobically with the ^{15}N-labeled frataxin orthologs show distinct alterations in α1 and β1 amino acid NMR resonances and, in the case of the CyaY and HsFtx, these perturbations are dependent on metal to protein stoichiometry. General trends in amide resonance perturbations upon addition of iron can be divided into two categories: amide resonances that were significantly line-broadened (often beyond detection), and amide chemical shifts that were shifted in the presence of metal. Bacterial amide resonances broadened upon addition of a single Fe(II) atom include α1 residues Arg20, Leu21, Asp22, and Asp23 (Table 1), while human resonances include α1 residues Asp112, Leu113, Asp115, and Val125 (Nair *et al.*, 2004). Additional bacterial resonances broadened upon the addition of a second Fe(II) atom include α1 residues Ser4, Glu5, Phe6, His7, Glu19 and Trp24,

TABLE 1 Comparison of the iron interaction with Yfh1, HsFtx and CyaY residues in α1 thru β2 secondary structural regions*.

Yfh1		HsFtx		CyaY		Structure Consensus
Sequence	Fe Effect	Sequence	Fe Effect	Sequence	Fe Effect	
Glu71		Thr93		Ser4	br2	
Lys72		Thr94		Glu5	br2	
Tyr73		Tyr95		Phe6	br2	α1
His74		Glu96		His7	br2	α1
Glu75	sh2	Arg97		Arg8		α1
Glu76	sh2	Leu98		Leu9		α1
Ala77		Ala99		Ala10		α1
Asp78	sh2	Glu100		Asp11		α1
Asp79	br2	Glu101		Gln12		α1
Tyr80		Thr102		Leu13		α1
Leu81		Leu103		Trp14		α1
Asp82	br2	Asp104	br2	Leu15		α1
His83	br2	Ser105		Thr16		α1
Leu84		Leu106		Ile17		α1
Leu85		Ala107	br2	Glu18		α1
Asp86	br2	Glu108	br2	Glu19	br2	α1
Ser87	sh2	Phe109		Arg20	br1	α1
Leu88		Phe110	br2	Leu21	br1	α1
Glu89	sh2	Glu111		Asp22	br1	α1
Glu90	sh2	Asp112	br1	Asp23	br1	α1
Leu91		Leu113	br1	Trp24	br2	
Ser92	sh2	Ala114	br2	Asp25		
Glu93	sh2	Asp115	br1	Gly26		
Ala94		Lys116		—		
—		Pro117		—		
His95		Tyr118		—		
Pro96		Thr119	br2	—		
Asp97		Phe120	br2	Asp27		
Cys98		Glu121		Ser28		
Ile99		Asp122	br2	Asp29		
Pro100		Tyr123		Ile30		
Asp101		Asp124	br2	Asp31	br2	β1
Val102		Val125	br1	Cys32	br2	β1
Glu103	br2	Ser126		Glu33		β1
Leu104		Phe127		Ile34		β1
Ser105	sh2	Gly128		Asn35		β1
His106		Ser129		Gly36		
Gly107		Gly130		Gly37		
Val108		Val131		Val38		β2
Met109		Leu132		Leu39		β2
Thr110		Thr133		Thr40		β2
Leu111	sh2	Val134		Ile41		β2
Glu112	br2	Lys135		Thr42		β2
Ile1113		Leu136		Phe43		β2

*The table represents a stoichiometry of between 1 to 2 Fe(II) per protein monomer. br1 and br2 (broadened and shifted at 1:1 and 2:1 respective Fe(II) to protein ratios) and sh2 (shifted at a 2:1 Fe(II) to protein). The final column contains the ortholog consensus secondary structure. The dashed line represents gaps in sequence homology (see Figure 2 for clarification).

K. Z. Bencze et al.

and $\beta 1$ residues Asp31 and Cys32; human resonances include $\alpha 1$ residues Asp104, Ala107, Glu108, Phe110, Ala114, Thr119, Phe120, Asp122, and Asp124. Addition of up to six Fe(II) atoms to CyaY and HsFtx caused a general broadening of amide resonances throughout the $\alpha 1$ and $\beta 1$ regions. A number of additional CyaY and HsFtx resonances in the $\alpha 1$ and $\beta 1$ regions underwent chemical shift perturbations upon the addition of ferrous metal. Yfh1 resonances broadened under similar buffer conditions by addition of up to two iron atoms include $\alpha 1$ residues Asp79, Asp82, His83, and Asp86, the $\beta 1$ residue Glu103 and the $\beta 2$ residue Glu112, while amide resonances for additional $\alpha 1$, $\beta 1$ and $\beta 2$ residues undergo chemical shift perturbations in the presence of iron (Cook *et al.*, 2006). Ferric iron titrations were performed on CyaY with similar results to those obtained from ferrous iron binding. CyaY residues significantly broadened at a 1:1 Fe(III) to protein stoichiometry include $\alpha 1$ residues Arg20, Asp22 and Asp23. In the presence of a 2:1 ratio, additional broadened resonances include $\alpha 1$ residue Asp29, as well as $\beta 1$ residues Ile30, Asp31, Cys32, Glu33, and Ile34. Again, addition of up to six iron atoms causes a general broadening of $\alpha 1$ and $\beta 1$ resonances. Finally binding studies performed on CyaY with the non-paramagnetic Ca(II) ions showed general chemical shift perturbations in only the $\alpha 1$ and $\beta 1$ regions (Nair *et al.*, 2004). In summary, these NMR titrations paint a picture of frataxin's metal binding residues located predominately in the conserved acidic $\alpha 1$ and $\beta 1$ regions of frataxin (Table 1).

Structural studies directed at characterizing the metal-ligand coordination geometry and electronic properties of bound iron provide additional insight into the metal binding ability of the monomeric frataxin orthologs. X-ray absorption spectroscopy (XAS) provides a powerful tool for characterizing structural and electronic properties of metals bound to proteins in solution (Teo, 1986). This technique has been used to characterize iron bound to Yfh1 and HsFtx monomers. Iron bound to monomeric Yfh1 and HsFtx is stable in the ferrous state when samples are prepared anaerobically or in the presence of the reducing agent dithionite (Bencze *et al.*, 2006; Cook *et al.*, 2006). Analysis of the iron 1s→3d transitions in the x-ray absorption near edge structure (XANES) portion of the XAS spectra are consistent with ferrous iron existing in the high-spin state and coordinated in a highly centrosymmetric metal-ligand coordination

geometry when bound to monomeric HsFtx and Yfh1 (Bencze *et al.*, 2006; Cook *et al.*, 2006). Structural analysis of the Fe(II)-ligand coordination geometry for monomeric Yfh1 and HsFtx from the extended x-ray absorption fine structure (EXAFS) portion of the XAS spectrum are consistent with iron bound in a highly symmetric six-coordinate ligand environment. Ligands coordinating Fe(II) are exclusively oxygen and/or nitrogen based, in agreement with $\alpha 1$ and $\beta 1$ Asp, Glu and His residues identified in the multiple NMR titrations as residues that possibly interact with iron. Additional ligands to the protein bound metal surely also come from water or hydroxide ions. There is no evidence for any metal–metal interaction for the ferrous iron bound to monomeric frataxin, even when up to two metals are bound in both Yfh1 and HsFtx.

Frataxin Can Form Stable Iron Loaded Homooligomers

Frataxin's ability to homooligomerize, forming aggregates with metal binding abilities similar to that of ferritin, suggests frataxin may act as an iron storage protein. Under elevated metal-to-protein stoichiometries, in the presence of oxygen and the absence of salt, Yfh1 will form a 48-multimeric homooligomer that can bind up to 50 iron atoms per protein monomer (Gakh *et al.*, 2002). CyaY aggregates of a similar size and iron loading capacity will also form under low-salt, aerobic, and iron-overloaded solution conditions (Adinolfi *et al.*, 2002). Assembly in both systems is predominately averted under high concentrations of other divalent metal ions or in the presence of physiological salt concentrations (Adamec *et al.*, 2000; Adinolfi *et al.*, 2002; Cook *et al.*, 2006), indicating CyaY and Yfh1 assembly is iron specific and will proceed under low salt but molecular oxygen (O$_2$) dependent conditions. Monomeric HsFtx does not self-assemble even at high iron concentrations, however a ~59-mer HsFtx homooligomer is isolated as part of the *Escherchia coli* overexpressed protein and this oligomer can bind approximately 10 iron atoms under aerobic and salt-free conditions (Cavadini *et al.*, 2002). The bulk iron bound in Yfh1 and HsFtx assemblies is predominately in the high-spin Fe(III) state (Nichol *et al.*, 2003).

Yfh1 homooligomers have a unique morphology that highly resemble those seen from the iron storage protein ferritin, suggesting iron storage may be

an important function of frataxin (Adamec *et al.*, 2000; Gakh *et al.*, 2002). Unlike ferritin, which forms spherical aggregates in the absence of metal (Theil, 1973), Yfh1 will only self-assemble in the presence of Fe, O_2, and low salt (Adinolfi *et al.*, 2002; Park *et al.*, 2002). Stoichiometric and higher Fe(II):protein ratios drive Yfh1 to progressively self-assemble into larger homooligomers beginning from a protein trimer repeating unit, directing next to a hexamer, then to a 12-mer, 24-mer and finally resulting in the 48-mer spherical protein aggregate that resembles ferritin (Adamec *et al.*, 2000). The 48-mer Yfh1 aggregate stores bulk metal, of greater than 2000 iron atoms, predominately as ferrihydrite (Nichol *et al.*, 2003). The ~59-mer HsFtx homooligomers, isolated from a portion of the protein overexpressed in *E. coli*, will store ~600 iron atoms as ferrihydrite in a rod-shaped polymeric protein structural morphology (Cavadini *et al.*, 2002). Non-covalent protein subunit interactions, mediated by the non-conserved N-terminal region of human frataxin, were shown to be important for assembly (O'Neill, Gakh *et al.*, 2005). Iron does not induce the assembly of the monomeric truncated portion of overexpressed HsFtx isolated from *E. coli* (Adinolfi *et al.*, 2002). CyaY can also form aggregates in the presence of iron and like Yfh1, aggregation is closely controlled by the presence of salt (Adinolfi *et al.*, 2002). Analytical ultracentrifugation studies show that CyaY tetramers can be formed when Fe(II) is added anaerobically; different protein aggregates are formed upon oxidation of the bound Fe(II) (Bou-Abdallah *et al.*, 2004). These *in vitro* assembly results are intriguing as they suggest protein aggregation may be an important property of the protein, in that it may help regulate cellular iron homeostasis under iron overloaded cellular conditions.

Residues in the $\alpha 1/\beta 1$ region are essential for controlling frataxin homooligomerization. Specific conserved acidic residues in the $\alpha 1/\beta 1$ region of Yfh1 and CyaY are required for assembly. Mutating CyaY $\alpha 1$ residues Glu18, Glu19, and Asp22, along with $\beta 1$ residue Glu33 abolishes the iron induced oligomerization behavior (Adinolfi *et al.*, 2002). Mutating conserved Yfh1 acidic residues Asp86, Glu90 and Asp93 abolishes the iron induced oligomerization behavior of the protein, surprisingly with no real *in vivo* phenotypes under normal growth conditions (Aloria *et al.*, 2004). Additional Yfh1 mutational studies indicate Asp93 is critical for protein self-assembly (Gakh *et al.*, 2006).

Unlike CyaY and Yfh1, a portion of the full-length mature HsFtx (residues 56 to 210) will self-assemble in the absence of metal; N-terminally truncated HsFtx lacking the initial 22 residues does not self assemble in the absence of iron (Cavadini *et al.*, 2002; O'Neill, Gakh *et al.*, 2005).

XAS results show iron bound to Yfh1 and HsFtx spherical aggregates is predominately stable in the ferric state when samples are prepared aerobically at high metal to protein ratios (Nichol *et al.*, 2003). Analysis of the 1s→3d transitions in the XANES spectra indicate ferric iron is coordinated in a highly centrosymmetric metal-ligand structural environment. Structural analysis of ferric iron coordinated to Yfh1 and HsFtx aggregates are consistent with bulk metal being bound as ferrihydrite, a biomineral composed of ferric oxide/hydroxide octahedra. The ligands coordinating the metal come predominately from complexed mono- and bidentate oxygen ligands that hold the multinuclear Fe cluster together and not from protein based ligands. These structural studies were essential for the early identification of how frataxin oligomers store bulk metal, hence participating as an iron storage capacity, maintaining metal in an inert form to shield the cell against unwanted iron redox chemistry.

Functional correlations between frataxin oligomers and ferritin are obvious. Mitochondrial ferritin (MtF) is an additional iron storage protein found in eukaryotes. Mature MtF is a 22 kDa protein encoded by an intronless gene on 5q23.1 chromosome in humans. MtF shares a 79% sequence identity with H-ferritin and the proteins possess ferroxidase activity. Its expression is restricted to tissues with high number of mitochondria (*i.e.*, the testis) unlike frataxin, which is ubiquitous in its expression. MtF expression is not correlated to tissues like liver, which are involved in iron storage. MtF expression is observed in iron-loaded erythroblasts from patients with sideroblastic anemia, but not in normal erythroblasts, suggesting it may be induced only under conditions of stress in some cells. Consistent with these data, reports show that MtF expression in normal cells results in cytoplasmic and mitochondrial iron deprivation and a decrease in enzymatic activity of Fe-S cluster containing enzymes like aconitase (Levi *et al.*, 2004). Correlating these findings with what is known about iron storage role of frataxin, it is possible that frataxin may be the iron storage molecule under low-salt but normal iron level conditions whereas both

K. Z. Bencze et al.

frataxin and mitochondrial ferritin scavenge iron to protect the cell from oxidative damage under iron overloading conditions.

Frataxin Controls Iron's Redox Chemistry

As previously outlined, iron is extremely reactive toward oxygen-based redox chemistry, so it is not surprising that a breakdown in cellular iron homeostasis resulting from a frataxin deficiency causes elevated oxidative stress to affected cells. Controlling the ability of iron to perform redox chemistry appears to be an additional function of frataxin, suggesting this protein may directly participate in controlling cellular oxidative stress by reducing ROS production. *In vivo* reports indicate frataxin deficiency leads to oxidative damage in humans (Emond *et al.*, 2000; Schultz *et al.*, 2000), mice (Ristow *et al.*, 2003; Thierbach *et al.*, 2005), yeast (Karthikeyan *et al.*, 2003), and *Caenorhabditis elegans* (Vazquez-Manrique *et al.*, 2006). Mitochondrial iron overload, resulting from a frataxin deficiency, leads to oxidative damage in mitochondrial and nuclear DNA as well as to Fe-S clusters in mitochondrial aconitase and other respiratory enzymes (Babcock *et al.*, 1997; Cavadini *et al.*, 2000; Foury, 1999; Karthikeyan *et al.*, 2002). Interestingly, frataxin affords protection for DNA against iron-induced oxidative damage (Gakh *et al.*, 2006; O'Neill *et al.*, 2005), presumably by directly binding iron and modulating its oxidation chemistry (Bou-Abdallah *et al.*, 2004).

In numerous biological systems, protein-controlled ferroxidase centers direct the controlled oxidation of ferrous iron. These centers are common among proteins within different metabolic pathways that involve iron. One of many examples of ferroxidase centers is found in the iron storage protein ferritin (Theil, 1987; Theil, 2003). Mammals contain two types of ferritin subunits, the heavy (H) chain and the light (L) chain, which differ in size. Ferritin binds ferrous iron *via* Glu and His residues on the H chain and metal is ultimately oxidized at the protein's ferroxidase center to form an oxygen bridged diferric center. Metal is then moved from the ferroxidase center to the nucleation site for storage as inert ferric oxide cores.

Recent reports have shown that frataxin will also perform ferroxidase chemistry (Park *et al.*, 2002). In Yfh1 at sub-stoichiometric metal to protein levels, cou-pled with ferrous iron oxidation, H_2O_2 is most likely generated through O_2 consumption during the ferroxidase reaction. The presence of hydrogen peroxide is only minimally detected under these conditions, and therefore it has been proposed that H_2O_2 immediately reacts with protein to attenuate all Fenton chemistry. Ferroxidation is progressively overcome by slower auto-oxidation at stoichiometric and higher iron to protein concentrations in Yfh1, and metal oxidation leads to progressive assembly of higher order protein oligomers. Therefore, it has been suggested that frataxin's ability to initially perform ferroxidase chemistry, retaining a portion of bound metal in a bioavailable form, and eventually storing iron in a less accessible form, allows this protein to serve both as an iron chaperone and an iron storage protein (Park *et al.*, 2003). Formation of the ferroxidase center in yeast frataxin is correlated to α1 residues Asp79 and Asp82; yeast mutants targeting these residues have reduced ferroxidase activity and assemble at a slower rate than wild type protein (Gakh *et al.*, 2006). A series of frataxin α1/β1 residues were implicated as participating in the iron mineralization chemistry observed under iron overloaded conditions, possibly by acting as iron binding amino acids in the yeast frataxin oligomers. Yfh1 residues α1 Asp86, Glu89, Glu90, and Glu93, and β1 residues Asp101 and Glu103 are generally important in promoting the iron binding and metal sequestering properties of frataxin oligomers (Gakh *et al.*, 2006).

Ferroxidase centers were also detected in HsFtx and CyaY aggregates (O'Neill *et al.*, 2005). The oligomeric form of iron loaded HsFtx showed distinct protection of DNA against oxidative damage in the presence of H_2O_2 (O'Neill *et al.*, 2005). Iron oxidation studies on CyaY monomers showed no apparent ferroxidase activity in the presence of molecular oxygen; rather, O_2 acted as a rather poor oxidant of Fe(II) bound to the protein (Bou-Abdallah *et al.*, 2004). The oxidation of Fe(II) bound to CyaY was accelerated in the presence of H_2O_2 and as a result there was an increase in the protein's ability to bind additional metals (Bou-Abdallah *et al.*, 2004). Unpublished results from our laboratory for Yfh1 monomers showed similar results to those published for CyaY monomers, with O_2-induced Fe(II) oxidation rates on the minutes time scale (50% conversion in ~10 minutes at 100 μm protein/iron concentrations). In these published studies, during the reduction of O_2 to $2H_2O$, the presence of highly reactive H_2O_2 or hydroxyl radicals was minimal.

FRATAXIN'S ROLE IN CELLULAR HEME BIOSYNTHESIS

Cells often utilize heme prosthetic groups when helping control normal cellular pathways. Given that frataxin is required for the production of heme, it is not a far stretch to suggest this protein could directly participate in heme bioassembly. Heme, a ubiquitous iron-containing tetrapyrrole ring system, is involved in multiple aspects of cellular metabolism. The Fe-prosthetic groups are used by globins, cytochromes and several additional enzymes (Ponka, 1999) that play key roles in the sensing and/or utilization of molecular oxygen in all living organisms (Andrew *et al.*, 1990; Padmanaban *et al.*, 1989; Zhu *et al.*, 1999). Heme centers help drive cellular energy generation during respiration by storing and transporting oxygen (Atamna, 2004). Heme groups can also participate in both catalytic and regulatory functions within cells (Zhu *et al.*, 2002). This prosthetic group can function as an effector center that regulates several biological processes encompassing transcription, translation, protein translocation and erythroid differentiation (Padmanaban *et al.*, 1989). They function as ligands for transcription factors within prokaryotes (Monson *et al.*, 1992) and in yeast (Creusot *et al.*, 1988; Fytlovich *et al.*, 1993; Pfeifer *et al.*, 1989; Zhang *et al.*, 1998). In higher eukaryotes, heme helps control the activity of specific transcription factors (Ogawa *et al.*, 2001; Sassa *et al.*, 1996) and proteins in several biochemical pathways by binding to the short protein sequence labeled the "heme regulatory motif" (Zhang *et al.*, 1995). Heme regulation is essential during erythroid differentiation. In mammalian erythroid cells, heme initiates changes in key factors controlling numerous activities ranging from cell cycle and Ras signaling to chromatin structure, splicing, and protein folding (Zhu *et al.*, 1999). Thus the multifunctional roles of heme suggests fluctuations in its concentration help control several key aspects of cellular metabolism (Atamna, 2004). In order to better understand the role frataxin plays in heme bioassembly, we present a brief description of the assembly pathway as it applies to our protein.

The heme biosynthetic pathway was outlined in detail during the 1950's and 60's (Labbe *et al.*, 1999). Cellular heme biosynthesis occurs in eight sequential steps, four of which (step 1 and steps 6 to 8) occur within the mitochondria, while the other steps occur within the cytoplasm (Tait, 1978). The enzyme ferrochelatase catalyses the final step in the heme biosynthetic pathway. Ferrous iron is inserted into porphyrin by ferrochelatase to produce a functional heme prosthetic group (Taketani, 2005). Ferrochelatase is associated with the inner mitochondrial membrane in eukaryotes; in prokaryotes, ferrochelatase is found within the cytoplasm (*Bacillus subtillus*) or associated to the cytoplasmic membrane (Dailey *et al.*, 2000). To this date, structures of apo- and metal-loaded bacterial (*Bacillus subtilis*), yeast (*Saccharomyces cerevisiae*), and human ferrochelatases have been solved (Al-Karadaghi *et al.*, 1997; Karlberg *et al.*, 2002; Wu *et al.*, 2001). While the functional bacterial protein is monomeric, human and yeast ferrochelatase are homodimers (Karlberg *et al.*, 2002). Mammalian, yeast (*Schizosaccharomyces pombe*) and some bacterial ferrochelatases are metalloenzymes that contain [2Fe-2S] prosthetic groups, which are required for activity (Ferreira, 1999). All three orthologs have a conserved overall fold of two Rossmann-type domains with a four-stranded parallel β-sheet that is flanked by α-helices. These domains contribute to the formation of the porphyrin-binding cleft. The differences between the eukaryotic and prokaryotic structures are mostly limited to the region in the eukaryotic ferrochelatase suggested to be involved in interactions with membranes and to the C-terminus, which contains the Fe-S cluster in the human but not the *S. cerevisiae* and *B. subtilis* enzymes (Karlberg *et al.*, 2002). The localization of ferrochelatase to the matrix side of the inner mitochondrial membrane ensures uptake of the poorly soluble porphyrin and heme release (Ferreira, 1999; Taketani, 2005). The hydrophobic exterior of ferrochelatase is in stark contrast to the hydrophilic interior of the active sites that are lined with conserved charged residues well positioned to receive the positively charged iron. The porphyrin-binding cleft of ferrochelatase exhibits a high degree of conservation from prokaryotes to higher eukaryotes (Al-Karadaghi *et al.*, 2006).

Ferrochelatase can chelate various divalent metal ions besides Fe^{2+}, most prominent being Zn^{2+} (Dailey, 2003). A general mechanism for the metallation of the tetrapyrrole, proposed in 1974, suggested that deformation of the porphyrin ring after an outer-sphere complex formation between the metal ion and porphyrin would generate an appropriate configuration for metal insertion (Hambright *et al.*, 1974). More recent studies have looked into mechanisms that endow ferrochelatase assisted ferrous ion metallation of

K. Z. Bencze et al.

porphyrin. Quantum and molecular mechanical calculations showed ferrochelatases induce a thermodynamically favorable distortion of free base protoporphyrin IX (Sigfridsson *et al.*, 2003). Al-Karadaghi and colleagues (2006) recently proposed that the degree of distortion imposed by ferrochelatase modulates the type of metal ion that is inserted, and this in turn is determined by subtle structural changes in the highly conserved active sites in the porphyrin binding cleft of ferrochelatase (Al-Karadaghi *et al.*, 2006).

Ferrochelatase requires ferrous iron as a substrate to complete heme assembly (Taketani, 2005) and the cellular mechanism that makes ferrous iron available, while also limiting the toxic effects of the metal, most likely involves the presence of a ferrous iron chaperone. Recent reports indicate that frataxin is the elusive iron chaperone that delivers the ferrous iron to ferrochelatase, hence promoting heme biosynthesis in a direct manner. In frataxin deleted yeast strains, Foury and colleagues (1997) observed a decrease in cytochrome c oxidase activity. Later Dancis and coworkers, working with frataxin null yeast strains, observed a severe deficiency of cytochromes b, c, and (a+a3) (Lesuisse *et al.*, 2003). Using a yeast strain with a single copy of Yfh1, placed under the control of a regulatable promoter to prevent rho minus conversion and secondary nuclear mutations that might mask the defect, the Dancis laboratory (University of Pennsylvania, Philadelphia) observed the recovery of cytochromes in general and cytochrome c in particular upon re-induction of frataxin expression (Lesuisse *et al.*, 2003). Although frataxin deleted cells have reduced levels of ferrochelatase, it was shown that cellular heme production is modulated by the insertion of zinc instead of iron into the porphyrin ring (Lesuisse *et al.*, 2003). Furthermore, increasing ferrochelatase levels using a multicopy plasmid did not correct the heme synthesis defect (Lesuisse *et al.*, 2003). These experiments proved that mitochondrial iron located in yeast frataxin deficient cells is not available for heme synthesis. Surface plasmon resonance studies showed, in the absence of iron, that recombinant Yfh1 interacts with yeast ferrochelatase with a high affinity ($K_d = 40$ nM) (Lesuisse *et al.*, 2003). Working toward obtaining a global result of frataxin deficiency, Schoenfeld and colleagues (2005) found that frataxin deficiency leads to the down regulation of mitochondrial transcripts and a kinetic inhibition of the heme pathway. An additional significant observation from their studies

was a large increase in zinc chelatase activity of ferrochelatase (Schoenfeld *et al.*, 2005), consistent with earlier studies by Lesuisse and coworkers (2003). This growing evidence implicates frataxin in determining the specificity of metal for the ferrochelatase by directly binding to the protein partner.

The presence of frataxin *in vitro* has been shown to stimulate heme development under controlled conditions. *In vitro* ferrochelatase activity assays, in the presence of citrate, showed that monomeric human frataxin can deliver the ferrous iron required for heme synthesis; an optimal ferrochelatase activity was observed at a stoichiometric ratio of one frataxin monomer per ferrochelatase dimer (Yoon *et al.*, 2004). The Cowan laboratory, using isothermal titration calorimetry and fluorescence quenching experiments, were able to quantitatively investigate complex formation between human frataxin and ferrochelatase. The K_d for the interaction between HsFtx and human ferrochelatase in the presence of iron was 17 nM; no interaction was detected for the human proteins in the absence of iron. In the yeast system, the Isaya laboratory showed ferrous iron associated with Yfh1 oligomers was available to yeast ferrochelatase for stimulation of *in vitro* heme synthesis (Park *et al.*, 2003). Metal transfer was shown to occur in the presence of Fe(II) specific chelators, suggesting again a strong intermolecular interaction is formed at the ferrous iron site in the frataxin-ferrochelatase protein complex (Park *et al.*, 2003).

Spectroscopic analysis of the yeast frataxin/ferrochelatase complex has been useful in helping to identify where and how the proteins interact. Our laboratory has shown that solution titrations, adding unlabeled yeast ferrochelatase into ^{15}N-labeled Yfh1, allowed us to probe by NMR which frataxin amino acids underwent amide chemical shift perturbations as a result of complex formation (He *et al.*, 2004). Frataxin chemical shift perturbations were localized predominantly on the helical plane of the protein. Specific Yfh1 residues affected by ferrochelatase binding included surface exposed α1 residues His83, Glu89, Glu90, Glu93 and His95, in the metal binding region of the protein (of which all Glu's are conserved), and β6-loop-α2 residues Val150, Asn154, Thr159, Asp160, Thr163, Glu164, Ser171, and Lys172 (of which Val150, Asn154, Thr163, and Glu164 are conserved in their physical properties). Yfh1 residues in the β6-loop region provide a hydrophobic patch on the protein and thus it is tempting to speculate that this domain

might help target and facilitate the binding of frataxin to the hydrophobic exterior of ferrochelatase (He et al., 2004). Complementary experiments were also performed on the human proteins by our laboratory in collaboration with the Cowan laboratory, with similar results identifying the helical residues perturbed upon complex formation (Bencze et al., 2006). These results suggest that the helical plane of frataxin, including the α1 iron-binding residues, is responsible for generating a favorable interface when frataxin binds to ferrochelatase.

Recently we performed modeling studies to predict how frataxin may interact with ferrochelatase. Using the Yfh1 solution structure (He et al., 2004) and the Co^{2+} bound yeast ferrochelatase crystal structure (Karlberg et al., 2002), we were able to generate a plausible model for the interaction between these two proteins (Figure 4) in an orientation that may suggest how iron is delivered to ferrochelatase during heme biosynthesis. We generated a large collection of complexes using the automatic docking program ZDOCK; however, we applied strict inclusion criteria that match published biophysical data when selecting appropriate docking interactions. The selection criteria utilized were: a) Yfh1 residues identified in our NMR titration as perturbed by the presence of ferrochelatase should be located at the interface, b) the location of the metal binding sites from both the human and yeast metal loaded ferrochelatase structures should face each other, and c) excluding the region of ferrochelatase that docks to the membrane (Wu et al., 2001). In our docking model, the Yfh1 monomer interacts with the yeast ferrochelatase dimer through highly conserved frataxin helices α1/α2 and the highly conserved ferrochelatase metal docking site including β4-loop-α6, α8 and α11 amino acids. Human ferrochelatase binds cobalt at this docking site using residues His231 and Asp383, located opposite to the membrane binding loops near a groove lined by arginines and lysines (Wu et al., 2001). These Lys and Arg residues could provide complementary electrostatic interactions to the acidic helices found in frataxin (Figure 1). In our docking model, the Yfh1 iron-binding α1 unit docks in close proximity to the ferrochelatase cobalt binding site found in the human ortholog; in yeast, two glutamate side chains are at this site and these could function during iron binding by the ferrochelatase. Iron bound to ferrochelatase would then be free to translocate towards the heme assembly active site (i.e., the position

of bound Co^{2+} in the *yeast* ferrochelatase structure), as has been proposed by Wu and colleagues (2001). These data are also consistent with the published ratio of 1:1 frataxin monomer/ferrochelatase dimer binding interactions seen in both the yeast and human systems (Lesuisse et al., 2003; Yoon et al., 2004). A recent report postulated protoporphyrin might help modulate the frataxin-ferrochelatase interaction, with porphyrin stabilizing the interaction (Al-Karadaghi et al., 2006). Porphyrin was, however, not added to our docking simulation. Given that the entry site for porphyrin is at the ferrochelatase surface opposite to the frataxin binding site, one would expect no direct effect of porphyrin binding on frataxin-ferrochelatase affinity. However, the lowest energy normal mode explored by free ferrochelatase, and the mode most likely to be physiologically relevant, shows that opening the porphyrin binding site partially closes the frataxin binding site. These results suggest a possible indirect effect on frataxin binding by ferrochelatase and *vice versa*. Current studies are underway in our laboratory to determine if iron or porphyrin alters the binding affinity between the wild type yeast frataxin and ferrochelatase proteins, and if mutating surface contact residues between the partners affects complex formation and metal transfer.

FRATAXIN AND Fe-S CLUSTER ASSEMBLY

Mounting evidence implicates frataxin as having a direct role in Fe-S cluster biosynthesis. Fe-S clusters are among the most complex and ancient prosthetic groups found in biology. They play essential roles in cellular processes ranging from electron transport, catalysis, gene regulation, and iron uptake (Chen et al., 2004). As an illustration of their importance, there are three separate pathways in bacteria for the production of Fe-S clusters. The first pathway identified involves the nitrogen fixation machinery that assembles the Fe-S clusters required for the maturation of nitrogenase (Frazzon et al., 2002; Rees et al., 2000). For most cellular needs, Fe-S clusters are provided by the second pathway, involving the ISC-assembly machinery (Kispal et al., 1999; Zheng et al., 1998). In some bacteria, a minor contributor under stressed conditions is the third pathway, the sulfur mobilization (SUF) machinery (Takahashi et al., 2002). Many bacteria contain more than one of these pathways, and interestingly they
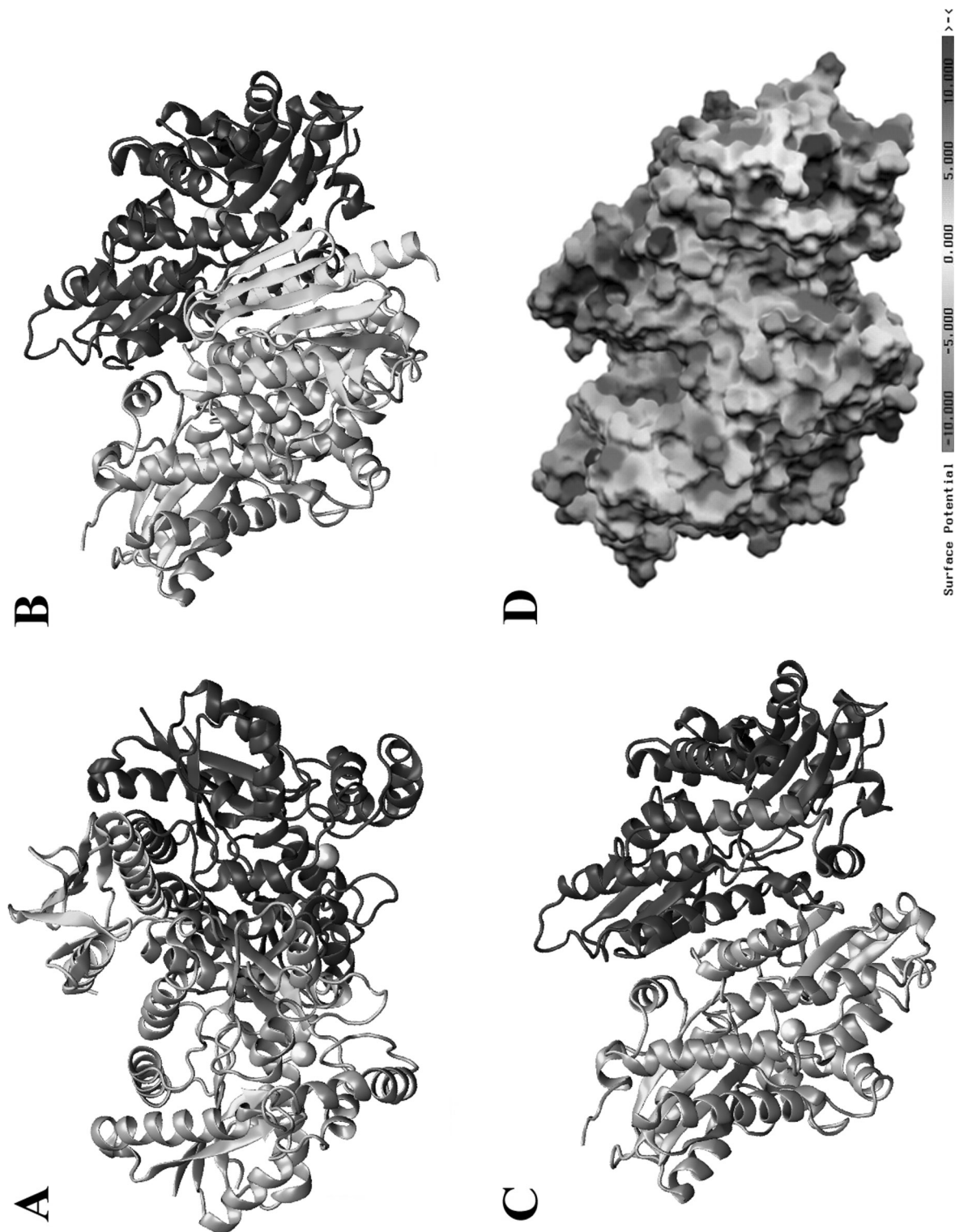
Figure 4 Lowest energy simulation of Yfh1 monomer docked to the metal loaded yeast ferrochelatase. (*A*) Side view of single Yfh1 monomer (green) docked to yeast ferrochelatase dimer (dark and light blue). Co^{2+} is bound in the yeast ferrochelatase structure in the assembly active site close to the four membrane attachment lips at the bottom of the figure. (*B*) Side view (90°—Horizontal rotation of Figure 4A) showing monomeric Yfh1 interacts with both units in the ferrochelatase dimer. (*C*) Ferrochelatase side view with Yfh1 structure removed to show the residues that directly interact with frataxin (in red). (*D*) Electrostatic potential plots (calculated and vendered with Grasp) of ferrochelatase, side view. Figures A, B, and C prepared using VMD (Humphry *et al*., 1996). Docking simulations were performed using ZDock (Chen *et al*., 2003) using the Yfh1 structure simulations (PDB ID# 2GA5) and Co^{2+} loaded yeast ferrochelatase structure (PDB ID# 1L8X). (Figure appears in color online at www.crbmb.com)

appear to be somewhat interchangeable (Ali *et al.*, 2004; Takahashi *et al.*, 2002). The mitochondria of eukaryotes however utilize only ISC orthologs for Fe-S cluster assembly and numerous reports outline the different characteristics of this highly important pathway (Johnson *et al.*, 2005; Lill *et al.*, 2005; Mansy *et al.*, 2004). A brief outline of the proteins within the yeast ISC-assembly machinery is given below as a basis for introducing frataxin's role in Fe-S cluster assembly.

Within the ISC-assembly pathway, yeast Fe-S cluster biosynthesis begins with the liberation of sulfur by the cysteine desulfurase, Nfs1 (Kispal *et al.*, 1999). A disulfide bond is formed between Nfs1 and free mitochondrial cysteine, leading to bond cleavage and alanine release (Lill *et al.*, 2005). Arh1, a ferredoxin reductase, and Yah1, a ferredoxin, are both required for efficient ISC assembly (Muhlenhoff *et al.*, 2003), and it has been proposed they provide the electrons necessary for sulfur liberation (Lill *et al.*, 2005). Next, sulfur is transferred to the cluster assembly scaffold proteins, a ~28 kDa protein dimer constructed of Isu1 (and/or) 2, usually *via* heterotetrameric complexes of the scaffold and the desulfurase (Garland *et al.*, 1999; Gerber *et al.*, 2003; Lill *et al.*, 2005; Schilke, 1999). The recently identified protein Isd11 is required to both stabilize and act as an adaptor between Nfs1, and the scaffold proteins, and this helps promote sulfur release (Adam *et al.*, 2006; Muhlenhoff *et al.*, 2003; Wiedemann *et al.*, 2006).

A general property of the scaffold proteins is that they are dynamic in nature, hence providing a flexible platform on which to construct Fe-S clusters while retaining the ability to release the prosthetic group for transfer to future acceptor proteins (Adinolfi *et al.*, 2004; Bertini *et al.*, 2003; Mansy *et al.*, 2004). While the structure of the yeast ortholog has not yet been solved, structures for Isu orthologs are consistent with having a β-sheet surface connected to a globular helical protein arrangement (Bertini *et al.*, 2003; Liu *et al.*, 2005; Ramelot *et al.*, 2004). The structure of Zn^{2+} bound to the *Streptococcus pyogenes* and *Haemophilus influenzae* orthologs shows that divalent metal is ligated by conserved cysteine residues in a surface exposed region of the protein monomer (Liu *et al.*, 2005; Ramelot *et al.*, 2004).

Frataxin is required for the *in vivo* production of Fe-S clusters and is believed to play a direct role in their assembly. A Fe-S cluster deficiency was identified in FRDA patients early in the recognition of the disorder,

suggesting the need for frataxin in Fe-S cluster assembly (Rotig *et al.*, 1997). This idea was supported by knockout mice showing similar disease phenotypes (Puccio *et al.*, 2001) and more recently in the bacterial system (Vivas C *et al.*, 2006). The majority of the direct frataxin *in vivo* Fe-S cluster correlations come again however from studies in the yeast system (Chen *et al.*, 2002; Duby *et al.*, 2002; Muhlenhoff *et al.*, 2002). Suppressing Yfh1 expression results in respiratory deficiency, mitochondrial iron accumulation and reduced Fe-S enzyme activity while non Fe-S containing enzymes remained active (Chen *et al.*, 2002). Additional studies suggest that frataxin may not be essential for Fe-S cluster assembly, but it does improve the efficiency of the assembly process (Duby *et al.*, 2002). A direct interaction between frataxin and the assembly apparatus proteins has been detected (Gerber *et al.*, 2003; Muhlenhoff *et al.*, 2003; Ramazzotti *et al.*, 2004), and the requirement of frataxin for the maturation of Fe-S clusters in yeast has been confirmed (Stehling *et al.*, 2004). Taken together, these data suggest frataxin plays a direct role in the cellular assembly of Fe-S clusters.

Recent *in vitro* studies show that frataxin binds to the ISU scaffold protein with high affinity and stimulates the production of Fe-S clusters, indicating that frataxin may be acting as the iron chaperone that delivers the Fe(II) required for bioassembly. Binding between *in vitro* human frataxin and the ISU dimer has been reported to occur with an affinity in the nanomolar range (Yoon *et al.*, 2003). Binding of monomeric HsFtx with the human ISU dimer was dependent on the presence of iron, in close correlation with yeast studies showing that the interaction between Yfh1 and Isu1/Nfs1 is also iron dependent (Gerber *et al.*, 2003). *In vitro* activity assays for the yeast and human protein systems show that the presence of frataxin stimulates Fe-S cluster assembly (Muhlenhoff, Richhardt, Gerber *et al.*, 2002; Yoon *et al.*, 2003). Based on the fact that frataxin is an iron-binding protein, that it binds tightly to the ISU complex and finally that it stimulates Fe-S cluster assembly, it seems highly probable that frataxin can act as the iron chaperone during Fe-S cluster bioassembly.

FRATAXIN ROLE IN ADDITIONAL PATHWAYS

Numerous reports have linked frataxin deficiency with an enhanced reduction in aconitase activity (Chen

K. Z. Bencze et al.

RIGHTS LINK()

et al., 2002; Foury, 1999; Rotig et al., 1997). Additional reports indicate frataxin may also deliver Fe(II) to aconitase for the use in repairing oxidatively damaged $[4Fe-4S]^{2+}$ clusters converted to the inactive $[3Fe-4S]^{+}$ form (Bulteau et al., 2004). Damage to aconitase, a Krebs-cycle enzyme that converts citrate to isocitrate (Beinert et al., 1996), has shown to be a marker for cellular oxidative damage (Bulteau et al., 2003). Reduced aconitase activity leads to increased transcription of the iron-import mechanism and this leads to further mitochondrial iron overload in FRDA patients (Chen et al., 2004). Frataxin interacts in a citrate dependent manner with oxidatively damaged aconitase, promoting aconitase enzyme reactivation suggesting frataxin delivers the Fe(II) required to reactivate the damaged iron-deficient Fe-S center (Bulteau et al., 2004). Furthermore, aconitase appears to directly associate with frataxin under high concentrations of ROS, possibly as a means to further protect aconitase against $[4Fe-4S]^{2+}$ cluster disassembly, irreversible inactivation, and potential degradation (Bulteau et al., 2005). ΔYfh1 yeast cells have low manganese superoxide-dismutase activity that can be recovered by supplementing Mn or limiting Fe in the media, suggesting a correlation between cellular iron overload and reduced SOD activity as a cause of oxidative stress in FRDA cells (Irazusta et al., 2006). Finally, the overexpression of frataxin in human cell lines leads to increased mitochondrial oxidative metabolism, as shown by an increased aconitase activity, mitochondrial membrane potential, cellular respiration, and ATP content (Schulz et al., 2006). These data suggest that frataxin provides a direct line of defense against cellular oxidative stress by controlling aconitase activity and iron import, as well as a possible additional indirect correlation between the partial regulation of the enzymatic activity of other proteins that control ROS activity.

OPEN QUESTIONS REGARDING FRATAXIN

Frataxin has been shown to play an important role in regulating cellular iron homeostasis, although the exact function(s) of the protein continues to remain controversial. While numerous groups have implicated frataxin as a protein that directs the utility of bioavailable iron, many key questions remain unanswered. If frataxin is an iron chaperone, what drives this chaperone to deliver iron specifically to multiple different protein partners (i.e., ferrochelatase, ISU scaffold or aconitase) when members of the copper chaperone family are highly specific with regard to their protein partners (Rosenzweig et al., 2000)? Certainly, additional structural data of frataxin in complex with each protein partner will help provide a better understanding of how and why these proteins interact within the different pathways. How can frataxin participate in two counterproductive roles, providing bioavailable and labile Fe(II,) when acting as an iron chaperone, while at other times retaining iron as inert Fe(III) when acting in an iron storage capacity, to help prevent toxicity? Structural data regarding iron-loaded frataxin oligomers will surely help address this issue of how and why these assemblies form, and identification of conditions when these assemblies can be observed in vivo will provide additional insight into their physiological relevance. Finally, what is the dominant function of frataxin? Recently frataxin has been shown to interact with the succinate dehydrogenase complex subunits, implying an additional possible role for frataxin in mitochondrial electron transport (Gonzalez-Cabo et al., 2005). Frataxin has also been shown to be a key activator of mitochondrial energy conversion and oxidative phosphorylation, suggesting yet another role for the protein in energy production (Ristow et al., 2000). Finally, CyaY has recently been shown to interact with the cysteine desulfurase IscS to promote both ferric iron reduction and Fe-S cluster assembly, suggesting iron delivery by frataxin may only occur when coupled with iron reduction (Layer et al., 2006). In vivo mutational studies that split the individual phenotypes for each pathway will provide biological relevance to help understand frataxin's role in each of the many functions proposed for this important protein. Addressing these and other equally important issues regarding how frataxin functions will surely help in developing improved treatment strategies to control iron regulation in disorders like Friedreich's ataxia.

REFERENCES

Adam, A.C., Bornhovd, C., Prokisch, H., Neupert, W., and Hell, K. 2006. The Nfs1 interacting protein Isd11 has an essential role in Fe/S cluster biogenesis in mitochondria. EMBO J 25:174.

Adamec, J., Rusnak, F., Owen, W.G., Naylor, S., Benson, L.M., Gacy, A.M., and Isaya, G. 2000. Iron-dependent self-assembly of recombinant yeast frataxin: implications for Friedreich ataxia. *Am J Hum Genet* 67:549.

Adinolfi, S., Trifuoggi, M., Politou, A.S., Martin, S., and Pastore, A. 2002. A structural approach to understanding the iron-binding properties of phylogenetically different frataxins. *Hum. Mol. Genet* 11:1865.

Adinolfi, S., Nair, M., Politou, A., Bayer, E., Martin, S., Temussi, P., and Pastore, A. 2004. The factors governing the thermal stability of frataxin orthologues: how to increase a protein's stability. *Biochemistry* 43:6511.

Adinolfi, S., Rizzo, F., Masino, L., Nair, M., Martin, S.R., Pastore, A., and Temussi, P.A. 2004. Bacterial IscU is a well folded and functional single domain protein. *Eur J Biochem* 271:2093.

Aisen, P., Enns, C., and Wessling-Resnick, M. 2001. Chemistry and biology of eukaryotic iron metabolism. *Int J Biochem Cell Biol* 33:940.

Al-Karadaghi, S., Hansson, M., Nikonov, S., Jonsson, B., and Hederstedt, L. 1997. Crystal structure of ferrochelatase: the terminal enzyme in heme biosynthesis. *Structure* 5:1501.

Al-Karadaghi, S., Franco, R., Hansson, M., Shelnutt, J.A., Isaya, G., and Ferreira, G.C. 2006. Chelatases: distort to select?. *Trends Biochem Sci* 31:135.

Ali, V., Shigeta, Y., Tokumoto, U., Takahashi, Y., and Nozaki, T. 2004. An intestinal parasitic protist, Entamoeba histolytica, possesses a non-redundant nitrogen fixation-like system for iron-sulfur cluster assembly under anaerobic conditions. *J Biol Chem* 279:16863.

Aloria, K., Schilke, B., Andrew, A., and Craig, E.A. 2004. Iron-induced oligomerization of yeast frataxin homologue Yfh1 is dispensable in vivo. *EMBO Rep* 5:1096.

Anastassopoulou, I., Banci, L., Bertini, I., Cantini, F., Katsari, E., and Rosato, A. 2004. Solution structure of the apo and copper(I)-loaded human metallochaperone HAH1. *Biochemistry* 43:13046.

Andrew, T.L., Riley, P.G., and Dailey, H.A. 1990. Regulation of heme biosynthesis in higher animals. In: Dailey, H.A. ed. *Biosynthesis of Heme and Cholorophylls*. New York: Green Pub. Associates and Wiley-Interscience, 183.

Andrews, N.C. 1999. Disorders of iron metabolism. *N Engl J Med* 341:1986.

Arnesano, F., Banci, L., Bertini, I., Huffman, D.L., and O'Halloran, T.V. 2001. Solution structure of the Cu(I) and apo forms of the yeast metallochaperone, Atx1. *Biochemistry* 40:1528.

Atamna, H. 2004. Heme, iron, and the mitochondrial decay of ageing. *Ageing Res Rev* 3:303.

Babcock, M., de Silva, D., Oaks, R., Davis-Kaplan, S., Jiralerspong, S., Montermini, L., Pandolfo, M., and Kaplan, J. 1997. Regulation of mitochondrial iron accumulation by Yfh1p, a putative homolog of frataxin. *Science* 276:1709.

Banci, L. and Bertini, I. 2003. Solution structure of apo CopZ from Bacillus subtilis: further analysis of the changes associated with the presence of copper. *Biochemistry* 42:13422.

Bartolo, C., Mendell, J.R., and Prior, T.W. 1998. Identification of a missense mutation in a Friedreich's ataxia patient: implications for diagnosis and carrier studies. *Am J Med Genet* 79:396.

Beinert, H., Kennedy, M.C., and Stout, C.D. 1996. Aconitase as ironminus signsulfur protein, enzyme, and iron-regulatory protein. *Chem Rev* 96:2335.

Bencze, K.Z., Yoon, T., Millán-Pacheco, C., Pastor, N., Cowan, J.A., and Stemmler, T.L. 2006. Human frataxin: Iron structure and ferrochelatase binding surface. *J Am Chem Soc* (Submitted)

Bertini, I., Cowan, J.A., Del Bianco, C., Luchinat, C., and Mansy, S.S. 2003. Thermotoga maritima IscU. Structural characterization and dynamics of a new class of metallochaperone. *J Mol Biol* 331:907.

Bidichandani, S.I., Ashizawa, T., and Patel, P.I. 1997. Atypical Friedreich ataxia caused by compound heterozygosity for a novel missense mutation and the GAA triplet-repeat expansion. *Am J Hum Genet* 60:1251.

Bidichandani, S.I., Ashizawa, T., and Patel, P.I. 1998. The GAA triplet-repeat expansion in Friedreich ataxia interferes with transcription and may be associated with an unusual DNA structure. *Am J Hum Genet* 62:111.

Bou-Abdallah, F., Adinolfi, S., Pastore, A., Laue, T.M., and Dennis Chasteen, N. 2004. Iron binding and oxidation kinetics in frataxin CyaY of *Escherichia coli*. *J Mol Biol* 341:605.

Branda, S.S., Yang, Z.Y., Chew, A., and Isaya, G. 1999. Mitochondrial intermediate peptidase and the yeast frataxin homolog together maintain mitochondrial iron homeostasis in *Saccharomyces cerevisiae*. *Hum Mol Genet* 8:1099.

Branda, S.S., Cavadini, P., Adamec, J., Kalousek, F., Taroni, F., and Isaya, G. 1999. Yeast and human frataxin are processed to mature form in two sequential steps by the mitochondrial processing peptidase. *J Biol Chem* 274:22763.

Bulteau, A.L., Ikeda-Saito, M., and Szweda, L.I. 2003. Redox-dependent modulation of aconitase activity in intact mitochondria. *Biochemistry* 42:14846.

Bulteau, A.L., Lundberg, K.C., Ikeda-Saito, M., Isaya, G., and Szweda, L.I. 2005. Reversible redox-dependent modulation of mitochondrial aconitase and proteolytic activity during in vivo cardiac ischemia/reperfusion. *Proc Natl Acad Sci U S A* 102:5987.

Bulteau, A.L., O'Neill, H.A., Kennedy, M.C., Ikeda-Saito, M., Isaya, G., and Szweda, L.I. 2004. Frataxin acts as an iron chaperone protein to modulate mitochondrial aconitase activity. *Science* 305:242.

Campuzano, V., Montermini, L., Molto, M.D., Pianese, L., Cossee, M., Cavalcanti, F., Monros, E., Rodius, F., Duclos, F., Monticelli, A., et al. 1996. Friedreich's ataxia: autosomal recessive disease caused by an intronic GAA triplet repeat expansion. *Science* 271:1423.

Cavadini, P., Gellera, C., Patel, P.I., and Isaya, G. 2000. Human frataxin maintains mitochondrial iron homeostasis in Saccharomyces cerevisiae. *Hum Mol Genet* 9:2523.

Cavadini, P., O'Neill, H.A., Benada, O., and Isaya, G. 2002. Assembly and iron-binding properties of human frataxin, the protein deficient in Friedreich ataxia. *Hum Mol Genet* 11:217.

Cavadini, P., Adamec, J., Taroni, F., Gakh, O., and Isaya, G. 2000. Two-step processing of human frataxin by mitochondrial processing peptidase. Precursor and intermediate forms are cleaved at different rates. *J Biol Chem* 275:41469.

Chen, O.S., Hemenway, S., and Kaplan, J. 2002. Inhibition of Fe-S cluster biosynthesis decreases mitochondrial iron export: evidence that Yfh1p affects Fe-S cluster synthesis. *Proc Natl Acad Sci U S A* 99:12321.

Chen, O.S., Crisp, R.J., Valachovic, M., Bard, M., Winge, D.R., and Kaplan, J. 2004. Transcription of the yeast iron regulon does not respond directly to iron but rather to iron-sulfur cluster biosynthesis. *J Biol Chem* 279:29513.

Chen, R., Li, L., and Weng, Z. 2003. ZDOCK: an initial-stage protein-docking algorithm. *Proteins* 52:80.

Cho, S.J., Lee, M.G., Yang, J.K., Lee, J.Y., Song, H.K., and Suh, S.W. 2000. Crystal structure of Escherichia coli CyaY protein reveals a previously unidentified fold for the evolutionarily conserved frataxin family. *Proc Natl Acad Sci U S A* 97:8932.

Cook, J.D., Bencze, K.Z., Jankovic, A.D., Crater, A.K., Busch, C.N., Bradley, P.B., Stemmler, A.J., Spaller, M.R., and Stemmler, T.L. 2006. Monomeric yeast frataxin is an iron binding protein. *Biochemistry* 45:7767.

Cossee, M., Durr, A., Schmitt, M., Dahl, N., Trouillas, P., Allinson, P., Kostrzewa, M., Nivelon-Chevallier, A., Gustavson, K.H., and Kohlschutter, A. 1999. Friedreich's ataxia: point mutations and clinical presentation of compound heterozygotes. *Ann Neurol* 45:200.

Cotton, F.A. and Wilkinson, G. 1988. *Advanced Inorganic Chemistry*. New York: John Wiley & Sons.

Creusot, F., Verdiere, J., Gaisne, M., and Slonimski, P.P. 1988. CYP1 (HAP1) regulator of oxygen-dependent gene expression in yeast. I. Overall organization of the protein sequence displays several novel structural domains. *J Mol Biol* 204(2):263.

Dailey, H.A., Dailey, T.A., Wu, C.K., Medlock, A.E., Wang, K.F., Rose, J.P., and Wang, B.C. 2000. Ferrochelatase at the millennium: structures, mechanisms and [2Fe-2S] clusters. *Cell Mol Life Sci* 57:1909.

Dailey, H.A. and T., A. 2003. Ferrochelatase. In: Kadish, K.M., Saith, K.M., Guilard, R., editors. *The Porphyrin handbook*. USA: Elsevier Science, 12:93.

Delatycki, M.B., Williamson, R., and Forrest, S.M. 2000. Friedreich ataxia: an overview. *J Med Genet* 37:1.

Dhe-Paganon, S., Shigeta, R., Chi, Y.I., Ristow, M., and Shoelson, S.E. 2000. Crystal structure of human frataxin. *J Biol Chem* 275:30753.

Duby, G., Foury, F., Ramazzotti, A., Herrmann, J., and Lutz, T. 2002. A non-essential function for yeast frataxin in iron-sulfur cluster assembly. *Hum Mol Genet* 11:2635.

Emond, M., Lepage, G., Vanasse, M., and Pandolfo, M. 2000. Increased levels of plasma malondialdehyde in Friedreich ataxia. *Neurology* 55:1752.

Ferreira, G.C. 1999. Ferrochelatase. *Int J Biochem Cell Biol* 31:995.

Filla, A., De Michele, G., Cavalcanti, F., Pianese, L., and Monticelli, A. 1996. The relationship between trinucleotide (GAA) repeat length and clinical features in Friedreich ataxia. *Am J Hum Genetics* 59: 554.

Forrest, S.M., Knight, M., Delatycki, M.B., Paris, D., Williamson, R., King, J., Yeung, L., Nassif, N., and Nicholson, G.A. 1998. The correlation of clinical phenotype in Friedreich ataxia with the site of point mutations in the FRDA gene. *Neurogenetics* 1:253.

Foury, F. 1999. Low iron concentration and aconitase deficiency in a yeast frataxin homologue deficient strain. *FEBS Letters* 456:281.

Foury, F. and Cazzalini, O. 1997. Deletion of the yeast homologue of the human gene associated with Friedreich's ataxia elicits iron accumulation in mitochondria. *FEBS Lett* 411:373.

Frazzon, J. and Dean, D.R. 2002. Biosynthesis of the nitrogenase iron-molybdenum-cofactor from Azotobacter vinelandii. *Met Ions Biol Syst* 39:163.

Fytlovich, S., Gervais, M., Agrimonti, C., and Guiard, B. 1993. Evidence for an interaction between the CYP1(HAP1) activator and a cellular factor during heme-dependent transcriptional regulation in the yeast Saccharomyces cerevisiae. *Embo J* 12:1209.

Gakh, O., Adamec, J., Gacy, A.M., Twesten, R.D., Owen, W.G., and Isaya, G. 2002. Physical evidence that yeast frataxin is an iron storage protein. *Biochemistry* 41:6798.

Gakh, O., Park, S., Liu, G., Macomber, L., Imlay, J.A., Ferreira, G.C., and Isaya, G. 2006. Mitochondrial iron detoxification is a primary function of frataxin that limits oxidative damage and preserves cell longevity. *Hum Mol Genet* 15:467.

Garland, S.A., Hoff, K., Vickery, L.E., and Culotta, V.C. 1999. Saccharomyces cerevisiae ISU1 and ISU2: members of a well-conserved gene family for iron-sulfur cluster assembly. *J Mol Biol* 294:897.

Gerber, J., Muhlenhoff, U., and Lill, R. 2003. An interaction between frataxin and Isu1/Nfs1 that is crucial for Fe/S cluster synthesis on Isu1. *EMBO Rep* 4:906.

Gibson, T.J., Koonin, E.V., Musco, G., Pastore, A., and Bork, P. 1996. Friedreich's ataxia protein: phylogenetic evidence for mitochondrial dysfunction. *Trends Neurosci* 19:465.

Gonzalez-Cabo, P., Vazquez-Manrique, R.P., Garcia-Gimeno, M.A., Sanz, P., and Palau, F. 2005. Frataxin interacts functionally with mitochondrial electron transport chain proteins. *Hum Mol Genet* 14: 2091.

Gordon, D.M., Wang, J., Amutha, B., and Pain, D. 2001. Self-association and precursor protein binding of Saccharomyces cerevisiae Tom40p, the core component of the protein translocation channel of the mitochondrial outer membrane. *Biochem J* 356:207.

Gordon, D.M., Kogan, M., Knight, S.A., Dancis, A., and Pain, D. 2001. Distinct roles for two N-terminal cleaved domains in mitochondrial import of the yeast frataxin homolog, Yfh1p. *Hum Mol Genet* 10:259.

Hambright, P. and Chock, P.B. 1974. Metal-porphyrin interactions. 3. A dissociative-interchange mechanism for metal ion incorporation into porphyrin molecules. *J Am Chem Soc* 96:3123.

He, Y., Alam, S.L., Proteasa, S.V., Zhang, Y., Lesuisse, E., Dancis, A., and Stemmler, T.L. 2004. Yeast frataxin solution structure, iron binding, and ferrochelatase interaction. *Biochemistry* 43:16254.

Humphry, W., Dalke, A., and Schulten, K. 1996. VMD—visual molecular dynamics. *J Molec Graphics* 14:33.

Irazusta, V., Cabiscol, E., Reverter-Branchat, G., Ros, J., and Tamarit, J. 2006. Manganese is the link between frataxin and iron-sulfur deficiency in the yeast model of Friedreich's ataxia. *J Biol Chem* 281:12227.

Johnson, D.C., Dean, D.R., Smith, A.D., and Johnson, M.K. 2005. Structure, function, and formation of biological iron-sulfur clusters. *Annu Rev Biochem* 74:247.

Karlberg, T., Lecerof, D., Gora, M., Silvegren, G., Labbe-Bois, R., Hansson, M., and Al-Karadaghi, S. 2002. Metal binding to Saccharomyces cerevisiae ferrochelatase. *Biochemistry* 41:13499.

Karthikeyan, G., Lewis, L.K., and Resnick, M.A. 2002. The mitochondrial protein frataxin prevents nuclear damage. *Hum Mol Genet* 11:1351.

Karthikeyan, G., Santos, J.H., Graziewicz, M.A., Copeland, W.C., Isaya, G., Van Houten, B., and Resnick, M.A. 2003. Reduction in frataxin causes progressive accumulation of mitochondrial damage. *Hum Mol Genet* 12:3331.

Kispal, G., Csere, P., Prohl, C., and Lill, R. 1999. The mitochondrial proteins Atm1p and Nfs1p are essential for biogenesis of cytosolic Fe/S proteins. *Embo J* 18:3981.

Knight, S.A., Sepuri, N.B., Pain, D., and Dancis, A. 1998. Mt-Hsp70 homolog, Ssc2p, required for maturation of yeast frataxin and mitochondrial iron homeostasis. *J Biol Chem* 273:18389.

Kosman, D.J. 2003. Molecular mechanisms of iron uptake in fungi. *Mol Microbiol* 47:1185.

Koutnikova, H., Campuzano, V., Foury, F., Dolle, P., Cazzalini, O., and Koenig, M. 1997. Studies of human, mouse and yeast homologues indicate a mitochondrial function for frataxin. *Nat Genet* 16:345.

Labbe, R.F., Vreman, H.J., and Stevenson, D.K. 1999. Zinc protoporphyrin: a metabolite with a mission. *Clin Chem* 45:2060.

Labuda, M., Poirier, J., and Pandolfo, M. 1999. A missense mutation (W155R) in an American patient with Friedreich ataxia. *Human Mutation* 13:506.

Layer, G., Ollagnier de Choudens, S., Sanakis, Y., and Fontecave, M. 2006. Iron-sulfur cluster biosynthesis: Characterization of Escherichia coli cyay as an iron donor for the assembly of [2Fe-2S] clusters in the scaffold ISCU. *J Biol Chem* 281:16256.

Lee, M.G., Cho, S.J., Yang, J.K., Song, H.K., and Suh, S.W. 2000. Crystallization and preliminary X-ray crystallographic analysis of Escherichia coli CyaY, a structural homologue of human frataxin. *Acta Crystallogr D Biol Crystallogr* 56(Pt 7):920.

Lesuisse, E., Santos, R., Matzanke, B.F., Knight, S.A., Camadro, J.M., and Dancis, A. 2003. Iron use for haeme synthesis is under control of the yeast frataxin homologue (Yfh1). *Hum Mol Genet* 12:879.

Levi, S. and Arosio, P. 2004. Mitochondrial ferritin. *Int J Biochem Cell Biol* 36:1887.

Lill, R. and Muhlenhoff, U. 2005. Iron-sulfur-protein biogenesis in eukaryotes. *Trends Biochem Sci* 30:133.

Liu, J., Oganesyan, N., Shin, D.H., Jancarik, J., Yokota, H., Kim, R., and Kim, S.H. 2005. Structural characterization of an iron-sulfur cluster assembly protein IscU in a zinc-bound form. *Proteins* 59: 875.

Mansy, S.S. and Cowan, J.A. 2004. Iron-sulfur cluster biosynthesis: toward an understanding of cellular machinery and molecular mechanism. *Acc Chem Res* 37:719.

Monson, E.K., Weinstein, M., Ditta, G.S., and Helinski, D.R. 1992. The FixL protein of Rhizobium meliloti can be separated into a heme-binding oxygen-sensing domain and a functional C-terminal kinase domain. *Proc Natl Acad Sci U S A* 89:4280.

Mori, S., Abeygunawardana, C., O'Neil Johnson, M., and van Zijl, P.C. 1995. Improved sensitivity of HSQC spectra of exchanging protons at short interscan delays using a new fast HSQC (FHSQC) detection scheme that avoids water saturation. *J Magn Res B* 108:94.

The Structure and Function of Frataxin

Muhlenhoff, U., Richhardt, N., Gerber, J., and Lill, R. 2002. Character-
ization of iron-sulfur protein assembly in isolated mitochondria.
A requirement for ATP, NADH, and reduced iron. *J Biol Chem*
277:29810.

Muhlenhoff, U., Gerber, J., Richhardt, N., and Lill, R. 2003. Components
involved in assembly and dislocation of iron-sulfur clusters on the
scaffold protein Isu1p. *EMBO J* 22:4815.

Muhlenhoff, U., Richhardt, N., Ristow, M., Kispal, G., and Lill, R. 2002. The
yeast frataxin homolog Yfh1p plays a specific role in the maturation
of cellular Fe/S proteins. *Hum Mol Genet* 11:2025.

Musco, G., Stier, G., Kolmerer, B., Adinolfi, S., Martin, S., Frenkiel, T.,
Gibson, T., and Pastore, A. 2000. Towards a structural understand-
ing of Friedreich's ataxia: the solution structure of frataxin. *Structure*
8:695.

Musco, G., de Tommasi, T., Stier, G., Kolmerer, B., Bottomley, M., Adinolfi,
S., Muskett, F.W., Gibson, T.J., Frenkiel, T.A., and Pastore, A. 1999.
Assignment of the 1H, 15N, and 13C resonances of the C-terminal
domain of frataxin, the protein responsible for Friedreich ataxia. *J
Biomol NMR* 15:87.

Nair, M., Adinolfi, S., Kelly, G., Frenkiel, T.A., and Pastore, A. 2003. NMR
assignment of the 1H, 15N and 13C resonances of the *E. coli*
frataxin orthologue, CyaY. *J Biomol NMR* 27:403.

Nair, M., Adinolfi, S., Pastore, C., Kelly, G., Temussi, P., and Pastore, A.
2004. Solution structure of the bacterial frataxin ortholog, CyaY:
mapping the iron binding sites. *Structure (Camb)* 12:2037.

Nichol, H., Gakh, O., O'Neill, H.A., Pickering, I.J., Isaya, G., and George,
G.N. 2003. Structure of frataxin iron cores: an X-ray absorption
spectroscopic study. *Biochemistry* 42:5971.

O'Neill, H.A., Gakh, O., and Isaya, G. 2005. Supramolecular assemblies
of human frataxin are formed via subunit-subunit interactions
mediated by a non-conserved amino-terminal region. *J Mol Biol*
345:433.

O'Neill, H.A., Gakh, O., Park, S., Cui, J., Mooney, S.M., Sampson, M.,
Ferreira, G.C., and Isaya, G. 2005. Assembly of human frataxin is a
mechanism for detoxifying redox-active iron. *Biochemistry* 44:537.

Ogawa, K., Sun, J., Taketani, S., Nakajima, O., Nishitani, C., Sassa,
S., Hayashi, N., Yamamoto, M., Shibahara, S., and Fujita, H.
2001. Heme mediates derepression of Maf recognition element
through direct binding to transcription repressor Bach1. *EMBO J* 20:
2835.

Ohshima, K., Montermini, L., Wells, R.D., and Pandolfo, M. 1998.
Inhibitory effects of expanded GAA.TTC triplet repeats from intron
I of the Friedreich ataxia gene on transcription and replication in
vivo. *J Biol Chem* 273:14588.

Orth, M. and Schapira, A.H. 2001. Mitochondria and degenerative
disorders. *Am J Med Genet* 106:27.

Padmanaban, G., Venkateswar, V., and Rangarajan, P.N. 1989. Haem as
a multifunctional regulator. *Trends Biochem Sci* 14:492.

Pandolfo, M. 2002. Iron metabolism and mitochondrial abnormalities in
Friedreich ataxia. *Blood Cells Mol Dis* 29:536.

Park, S., Gakh, O., Mooney, S.M., and Isaya, G. 2002. The ferroxidase
activity of yeast frataxin. *J Biol Chem* 277:38589.

Park, S., Gakh, O., O'Neill, H.A., Mangravita, A., Nichol, H., Ferreira,
G.C., and Isaya, G. 2003. Yeast frataxin sequentially chaperones
and stores iron by coupling protein assembly with iron oxidation. *J
Biol Chem* 278:31340.

Pfeifer, K., Kim, K.S., Kogan, S., and Guarente, L. 1989. Func-
tional dissection and sequence of yeast HAP1 activator. *Cell* 56:
291.

Ponka, P. 1999. Cell biology of heme. *Am J Med Sci* 318:241.

Puccio, H., Simon, D., Cossee, M., Criqui-Filipe, P., Tiziano, F., Melki, J.,
Hindelang, C., Matyas, R., Rustin, P., and Koenig, M. 2001. Mouse
models for Friedreich ataxia exhibit cardiomyopathy, sensory nerve
defect and Fe-S enzyme deficiency followed by intramitochondrial
iron deposits. *Nat Genet* 27:181.

Radisky, D.C., Babcock, M.C., and Kaplan, J. 1999. The yeast frataxin
homologue mediates mitochondrial iron efflux: evidence for a
mitochondrial iron cycle. *J Biol Chem* 274:4497.

Ramazzotti, A., Vanmansart, V., and Foury, F. 2004. Mitochondrial
functional interactions between frataxin and Isu1p, the iron-sulfur
cluster scaffold protein, in Saccharomyces cerevisiae. *FEBS Lett*
557:215.

Ramelot, T.A., Cort, J.R., Goldsmith-Fischman, S., Kornhaber, G.J., Xiao,
R., Shastry, R., Acton, T.B., Honig, B., Montelione, G.T., and
Kennedy, M.A. 2004. Solution NMR structure of the iron-sulfur
cluster assembly protein U (IscU) with zinc bound at the active site.
J Mol Biol 344:567.

Rees, D.C. and Howard, J.B. 2000. Nitrogenase: standing at the
crossroads. *Curr Opin Chem Biol* 4:559.

Ristow, M., Pfister, M.F., Yee, A.J., Schubert, M., Michael, L., Zhang,
C.Y., Ueki, K., Michael, M.D., Lowell, B.B., and Kahn, C.R. 2000.
Frataxin activates mitochondrial energy conversion and oxidative
phosphorylation. *Proc Natl Acad Sci U S A* 97:12239.

Ristow, M., Mulder, H., Pomplun, D., Schulz, T.J., Muller-Schmehl, K.,
Krause, A., Fex, M., Puccio, H., Muller, J., Isken, F., *et al.* 2003.
Frataxin deficiency in pancreatic islets causes diabetes due to loss
of beta cell mass. *J Clin Invest* 112:527.

Rosenzweig, A.C. and O'Halloran, T.V. 2000. Structure and chemistry of
the copper chaperone proteins. *Curr Opin Chem Biol* 4:140.

Rotig, A., de Lonlay, P., Chretien, D., Foury, F., Koenig, M., Sidi, D.,
Munnich, A., and Rustin, P. 1997. Aconitase and mitochondrial
iron-sulphur protein deficiency in Friedreich ataxia. *Nat Genet*
17:215.

Sassa, S. and Nagai, T. 1996. The role of heme in gene expression. *Int J
Hematol* 63:167.

Sazanov, L.A. and Hinchliffe, P. 2006. Structure of the hydrophilic domain
of respiratory complex I from Thermus thermophilus. *Science*
311:1430.

Schilke, B., Voisine, C., Beinert, H., and Craig, E. 1999. Evidence for
a conserved system for iron metabolism in the mitochondria of
Saccharomydes cervisiae. *Proc Natl Acad Sci USA* 96:10206.

Schoenfeld, R.A., Napoli, E., Wong, A., Zhan, S., Reutenauer, L., Morin,
D., Buckpitt, A.R., Taroni, F., Lonnerdal, B., Ristow, M., *et al.* 2005.
Frataxin deficiency alters heme pathway transcripts and decreases
mitochondrial heme metabolites in mammalian cells. *Hum Mol
Genet* 14:3787.

Schultz, J.B., Dehmer, T., Schols, L., Mende, H., Hardt, C., Vorgerd, M.,
Burk, K., Matson, W., Dichgans, J., and Beal, M.F. 2000. Oxidative
stress in patients with Friedreich's ataxia. *Neurology* 55:1719.

Schulz, T.J., Thierbach, R., Voigt, A., Drewes, G., Mietzner, B., Steinberg,
P., Pfeiffer, A.F., and Ristow, M. 2006. Induction of oxidative
metabolism by mitochondrial frataxin inhibits cancer growth: Otto
Warburg revisited. *J Biol Chem* 281:977.

Sigfridsson, E. and Ryde, U. 2003. The importance of porphyrin distortions
for the ferrochelatase reaction. *J Biol Inorg Chem* 8:273.

Stehling, O., Elsasser, H.P., Bruckel, B., Muhlenhoff, U., and Lill, R.
2004. Iron-sulfur protein maturation in human cells: evidence for a
function of frataxin. *Hum Mol Genet* 13:3007.

Tait, G.H. 1978. The Biosynthesis and degradation of heme. In: De
Matteis, F., Aldridge, N.W., editors. *Heme and Hemoproteins*.
Berlin: Springer-Verlag, pp. 1–35.

Takahashi, Y. and Tokumoto, U. 2002. A third bacterial system for the
assembly of iron-sulfur clusters with homologs in archaea and
plastids. *J Biol Chem* 277:28380.

Taketani, S. 2005. Aquisition, mobilization and utilization of cellular
iron and heme: endless findings and growing evidence of tight
regulation. *Tohoku J Exp Med* 205:297.

Teo, B.K. 1986. *EXAFS: Basic Principles and Data Analysis*. New York:
Springer-Verlag.

Theil, E.C. 1973. Amphibian red blood cell ferritin. *J Biol Chem* 248:622.

Theil, E.C. 1987. Ferritin: structure, gene regulation, and cellular function
in animals, plants, and microorganisms. *Annu Rev Biochem* 56:289.

Theil, E.C. 2003. Ferritin: at the crossroads of iron and oxygen metabolism.
J Nutr 133:1549S.

Thierbach, R., Schulz, T.J., Isken, F., Voigt, A., Mietzner, B., Drewes, G.,
von Kleist-Retzow, J.C., Wiesner, R.J., Magnuson, M.A., and Puccio,

H. 2005. Targeted disruption of hepatic frataxin expression causes impaired mitochondrial function, decreased life span and tumor growth in mice. *Hum Mol Genet* 14:3857.

Vazquez-Manrique, R.P., Gonzalez-Cabo, P., Ros, S., Aziz, H., Baylis, H.A., and Palau, F. 2006. Reduction of Caenorhabditis elegans frataxin increases sensitivity to oxidative stress, reduces lifespan, and causes lethality in a mitochondrial complex II mutant. *Faseb J* 20: 172.

Vivas, E., Skovran, E., and Downs, D.M. 2006. Salmonella enterica strains lacking the frataxin homolog CyaY show defects in Fe-S cluster metabolism in vivo. *J Bacteriol* 188:1175.

Wiedemann, N., Urzica, E., Guiard, B., Muller, H., Lohaus, C., Meyer, H.E., Ryan, M.T., Meisinger, C., Muhlenhoff, U., and Lill, R. 2006. Essential role of Isd11 in mitochondrial iron-sulfur cluster synthesis on Isu scaffold proteins. *EMBO J* 25:184.

Wu, C.K., Dailey, H.A., Rose, J.P., Burden, A., Sellers, V.M., and Wang, B.C. 2001. The 2.0 A structure of human ferrochelatase, the terminal enzyme of heme biosynthesis. *Nat Struct Biol* 8:156.

Yoon, T. and Cowan, J.A. 2003. Iron-sulfur cluster biosynthesis. Characterization of frataxin as an iron donor for assembly of [2Fe-2S] clusters in ISU-type proteins. *J Am Chem Soc* 125:6078.

Yoon, T. and Cowan, J.A. 2004. Frataxin-mediated iron delivery to Ferrochelatase in the final step of Heme biosynthesis. *J Biol Chem* 279:25943.

Zhang, L. and Guarente, L. 1995. Heme binds to a short sequence that serves a regulatory function in diverse proteins. *EMBO J* 14: 313.

Zhang, L., Hach, A., and Wang, C. 1998. Molecular mechanism governing heme signaling in yeast: a higher-order complex mediates heme regulation of the transcriptional activator HAP1. *Mol Cell Biol* 18:3819.

Zheng, L., Cash, V.L., Flint, D.H., and Dean, D.R. 1998. Assembly of iron-sulfur clusters. Identification of an iscSUA-hscBA-fdx gene cluster from Azotobacter vinelandii. *J Biol Chem* 273:13264.

Zhu, Y., Hon, T., and Zhang, L. 1999. Heme initiates changes in the expression of a wide array of genes during the early erythroid differentiation stage. *Biochem Biophys Res Commun* 258:87.

Zhu, Y., Hon, T., Ye, W., and Zhang, L. 2002. Heme deficiency interferes with the Ras-mitogen-activated protein kinase signaling pathway and expression of a subset of neuronal genes. *Cell Growth Differ* 13:431.

Zuhlke, C.H., Dalski, A., Habeck, M., Straube, K., Hedrich, K., Hoeltzenbein, M., Konstanzer, A., Hellenbroich, Y., and Schwinger, E. 2004. Extension of the mutation spectrum in Friedreich's ataxia: detection of an exon deletion and novel missense mutations. *Eur J Hum Genet* 12:979.

Editor: Elizabeth Craig